ADVANCED FUNCTIONAL MATERIALS

Supporting Information

for

Advanced Functional Materials, adfm.200600855

Optical Power Limiters Based on Colorless Di-, Oligo- and Polymetallaynes. Highly Transparent Materials for Eye Protection Devices

By Gui-Jiang Zhou, Wai-Yeung Wong, Cheng Ye, and Zhenyang Lin*

Synthesis and Characterization Data. In the shortform of each formula, the triple bonds are abbreviated by T and dioctylfluorene by C_8-F. Model complexes and polymers are differentiated by use of the subscripts 1 and n, respectively. The compounds **[H-T(C_8-F)T-H]$_1$**, **[T(C_8-F)T]$_n$**, **[Pt-T(C_8-F)T-Pt]$_1$**, **[Hg-T(C_8-F)T-Hg]$_1$**, **[Pt-T(C_8-F)T]$_n$** and **[Hg-T(C_8-F)T]$_n$** were prepared according to the published procedures.[1, 2]

[T(C_8-F)T-Pt-T(C_8-F)T]$_1$

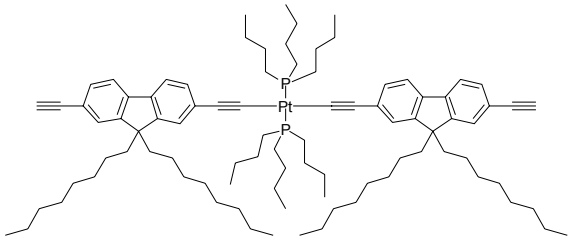

A solution of *trans*-[$PtCl_2(PBu_3)_2$] (0.153 g, 0.228 mmol) in CH_2Cl_2 (20 mL) was added slowly to a mixture of excess **[H-T(C_8-F)T-H]$_1$** (0.40 g, 0.913 mmol) and CuI (2 mg) in NEt_3/CH_2Cl_2 (150 mL, 1:1, v/v) at ambient temperature. After the addition, the reaction mixture was stirred at room temperature overnight. Following the filtration to remove the CuI catalyst residue, the filtrate was concentrated. The crude product was purified by column chromatography with hexane/CH_2Cl_2 (3:1, v/v) as eluent. The product was obtained as an off-white crystalline solid (0.235 g, 70%). IR (KBr): ν(C≡C) 2093 cm^{-1}. ^{1}H NMR (400 MHz, $CDCl_3$): δ = 7.55 (d, J = 7.6 Hz, 2H, Ar), 7.51 (d, J = 8.0 Hz, 2H, Ar), 7.45–7.42 (m, 4H, Ar), 7.24 (d, J = 8.4 Hz, 4H, Ar), 3.13 (s, 2H, C≡CH), 2.20 (m, 12H, PBu_3), 1.89 (m, 8H, C_8H_{17}), 1.65 (m, 12H, PBu_3), 1.48 (m, 12H, PBu_3), 1.22–1.12 (m, 40H, C_8H_{17}), 0.95 (t, J = 7.2 Hz, 18H, PBu_3), 0.83 (t, J = 7.2 Hz, 12H, C_8H_{17}), 0.57 ppm (br, 8H, C_8H_{17}). ^{13}C NMR (100.3 MHz, $CDCl_3$): δ = 150.53, 141.92, 137.12, 130.97, 129.62, 128.11, 126.23, 125.09,

119.46, 119.23, 119.07 (Ar), 108.84, 100.45, 84.88, 76.72 (C≡C) 54.85 (quat. C), 40.54, 31.83, 30.18, 29.36, 23.79, 22.66, 14.17 (C_8H_{17}), 26.47, 24.53, 24.08, 13.94 ppm (PBu_3). ^{31}P NMR (161.9 MHz, $CDCl_3$): δ = 4.02 ppm ($^1J_{P-Pt}$ = 2348 Hz). FAB-MS: *m/z* 1475 $[M]^+$. Anal. Calcd for $C_{90}H_{136}P_2Pt$: C, 73.28; H, 9.29. Found: C, 73.12; H, 9.08.

[T(C_8-F)T-Hg-T(C_8-F)T]$_1$

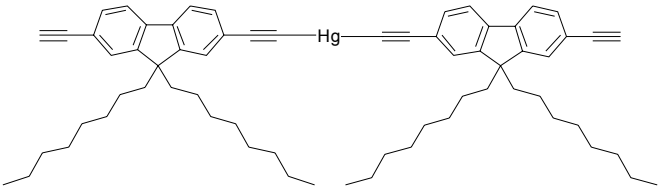

A basic solution of NaOMe (2.3 mL, 0.2 mmol/L in MeOH) was added slowly to a solution of **[H-T(C_8-F)T-H]$_1$** (0.40 g, 0.913 mmol) in MeOH/CH_2Cl_2 (150 mL, 10:1, v/v). Then, $HgCl_2$ (0.062 g, 0.229 mmol) in MeOH (15 mL) was added dropwisely to the as-prepared solution. The reaction mixture turned milky. After stirring overnight at ambient temperature, the precipitate formed was collected and purified by preparative TLC plates with hexane/CH_2Cl_2 (3:1, v/v) as eluent. The desired product was obtained as a pale yellow oil (0.148 g, 60%). IR (KBr): ν(C≡C) 2140 cm^{-1}. ^1H NMR (400 MHz, $CDCl_3$): δ = 7.61 (d, *J* = 7.2 Hz, 4H, Ar), 7.50–7.47 (m, 8H, Ar), 3.15 (s, 2H, C≡CH), 1.95 (m, 8H, C_8H_{17}), 1.22–1.03 (m, 40H, C_8H_{17}), 0.83 (t, *J* = 7.2 Hz, 12H, C_8H_{17}), 0.59 ppm (br, 8H, C_8H_{17}). ^{13}C NMR (100.3 MHz, $CDCl_3$): δ = 151.07, 151.04, 140.93, 131.49, 131.22, 126.70, 126.49, 121.01, 120.84, 120.80, 120.02, 119.97 (Ar), 106.88, 84.50, 77.38 (C≡C) 55.17 (quat. C), 40.22, 31.37, 29.94, 29.20, 23.65, 22.56, 14.08 ppm (C_8H_{17}). FAB-MS: *m/z* 1075 $[M]^+$. Anal. Calcd (%) for $C_{66}H_{82}Hg$: C, 73.68; H, 7.68. Found: C, 73.54; H, 7.48.

[Au-T(C_8-F)T-Au]$_1$

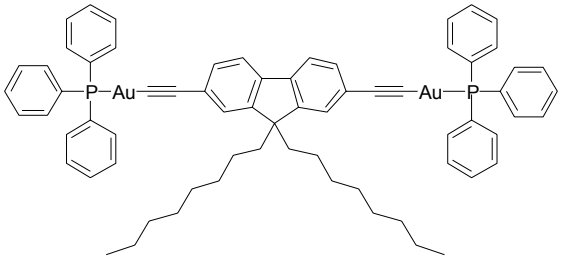

To a solution mixture of **[H-T(C_8-F)T-H]$_1$** (0.10 g, 0.228 mmol) and Au(PPh_3)Cl (0.25 g, 0.502 mmol) in MeOH (50 mL), NaOMe solution (2.5 mL, 0.2 mmol/L in MeOH) was added with a syringe. The reaction mixture was stirred overnight. The white precipitate was collected and washed with MeOH. Then, the product was purified by reprecipitating its concentrated CH_2Cl_2 solution from MeOH. The product as a white solid was collected and dried under vacuum (0.236 g, 77 %). IR (KBr): ν(C≡C) 2100 cm^{-1}. ^{1}H NMR (400 MHz, $CDCl_3$): δ = 7.59–7.43 (m, 36H, Ar), 1.87 (m, 4H, C_8H_{17}), 1.22–0.97 (m, 20H, C_8H_{17}), 0.81 (t, J = 7.2 Hz, 6H, C_8H_{17}), 0.53 ppm (br, 4H, C_8H_{17}). ^{13}C NMR (100.3 MHz, $CDCl_3$): δ = 150.61, 139.76, 134.24, 131.52, 131.04, 130.01, 129.46, 129.06, 126.96, 122.82 (Ar), 119.28, 105.32 (C≡C) 54.84 (quat. C), 40.63, 31.74, 30.16, 29.34, 29.32, 23.70, 22.54, 14.09 ppm (C_8H_{17}). ^{31}P NMR (161.9 MHz, $CDCl_3$): δ = 43.42 ppm. FAB-MS: *m/z* 1356 $[M]^+$. Anal. Calcd (%) for $C_{69}H_{70}Au_2P_2$: C, 61.15; H, 5.21. Found: C, 60.98; H, 5.04.

[Pt-T(C_8-F)T-Pt-T(C_8-F)T-Pt]$_1$

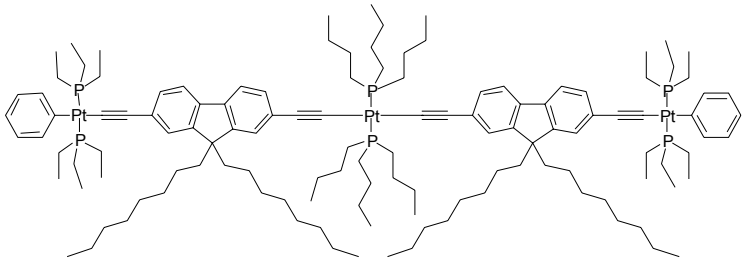

[T(C_8-F)T-Pt-T(C_8-F)T]$_1$ (0.15 g, 0.102 mmol) and *trans*-[PtCl(Ph)(PEt_3)$_2$] (0.12 g, 0.221 mmol) were dissolved in NEt_3/CH_2Cl_2 (50 mL, 1:1 v/v) at room temperature and a small amount of CuI was

then added. After the reaction mixture was stirred at room temperature overnight, it was filtered through a short silica gel pad. The filtrate was concentrated and the residue was separated by preparative TLC eluting with hexane/CH_2Cl_2 (2:1, v/v). The product was obtained as a viscous oil (0.19 g, 75%). IR (KBr): ν(C≡C) 2096 cm^{-1}. ^1H NMR (400 MHz, $CDCl_3$): δ = 7.46 (d, J = 3.2 Hz, 2H, Ar), 7.40 (d, J = 2.8 Hz, 2H, Ar), 7.34 (d, J = 7.2 Hz, 4H, Ar), 7.25–7.20 (m, 8H, Ar), 6.97 (t, J = 7.6 Hz, 4H, Ar), 6.82 (t, J = 7.2 Hz, 2H, Ar), 2.22–2.18 (m, 12H, PBu_3 and C_8H_{17}), 1.89–1.75 (m, 32H, PEt_3 and C_8H_{17}), 1.67–1.64 (m, 12H, PBu_3), 1.50–1.45 (m, 12H, PBu_3), 1.25–1.00 (m, 76H, PEt_3 and C_8H_{17}), 0.95 (t, J = 7.2 Hz, 18H, PBu_3), 0.83 (t, J = 7.2 Hz, 12H, C_8H_{17}), 0.65 ppm (br, 8H, C_8H_{17}). ^{13}C NMR (100.3 MHz, $CDCl_3$): δ = 156.43, 150.30, 139.15, 138.32, 138.09, 136.74, 129.68, 129.48, 127.83, 127.25, 127.15, 126.78, 125.23, 125.14, 121.19, 118.72 (Ar), 112.84, 111.58, 110.31, 107.67 (C≡C) 54.43 (quat. C), 40.63, 31.80, 30.25, 29.39, 29.35, 23.75, 22.57, 13.85 (C_8H_{17}), 26.36, 24.45, 23.93, 14.08 (PBu_3), 15.12, 7.78 ppm (PEt_3). ^{31}P NMR (161.9 MHz, $CDCl_3$): δ = 10.70 ($^1J_{P–Pt}$ = 2638 Hz, PEt_3), 3.81 ppm ($^1J_{P–Pt}$ = 2353 Hz, PBu_3). FAB-MS: *m/z* 2490 $[M]^+$. Anal. Calcd (%) for $C_{126}H_{204}P_6Pt_3$: C, 60.78; H, 8.26; Found: C, 60.55; H, 8.02.

[Hg-T(C_8-F)T-Hg-T(C_8-F)T-Hg]$_1$

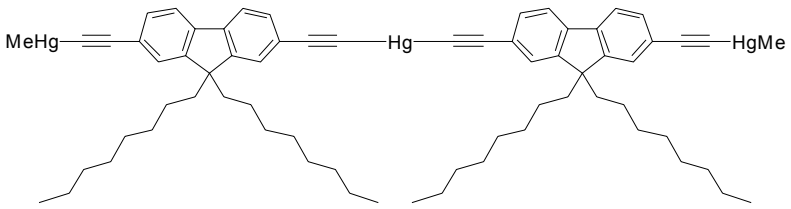

To a mixture of **[T(C_8-F)T-Hg-T(C_8-F)T]$_1$** (0.12 g, 0.112 mmol) and MeHgCl (0.070 g, 0.279 mmol) in CH_2Cl_2/MeOH (50 mL, 50:1, v/v), NaOMe solution (1.5 mL, 0.2 mmol/L in MeOH) was added. The reaction mixture was stirred overnight after which time the reaction mixture was concentrated

and the residue was purified by preparative TLC plates using hexane/CH_2Cl_2 (2:1, v/v) as eluent. The product was obtained as a white solid after drying under vacuum (0.116 g, 69%). IR (KBr): ν(C≡C) 2123 cm^{-1}. ^1H NMR (400 MHz, $CDCl_3$): δ = 7.57 (d, J = 8.4 Hz, 4H, Ar), 7.45–7.42 (m, 8H, Ar), 1.94–1.88 (m, 8H, C_8H_{17}), 1.25–1.01 (m, 40H, C_8H_{17}), 0.82 (t, J = 7.0 Hz, 12H, C_8H_{17}), 0.70 (s, 6H, HgMe), 0.55 ppm (br, 8H, C_8H_{17}). FAB-MS: m/z 1505 $[M]^+$. Anal. Calcd (%) for $C_{68}H_{86}Hg_3$: C, 54.26; H, 5.76. Found: C, 54.14; H, 5.43.

[Pt-T(C_8-F)T-Hg-T(C_8-F)T-Pt]$_1$

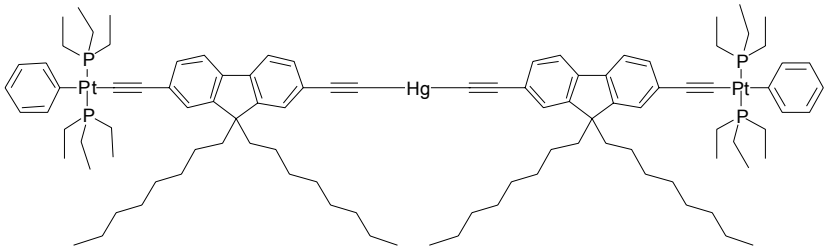

[T(C_8-F)T-Hg-T(C_8-F)T]$_1$ (0.10 g, 0.0929 mmol) and *trans*-[PtCl(Ph)(PEt_3)$_2$] (0.126 g, 0.232 mmol) were added to a mixture of NEt_3/CH_2Cl_2 (40 mL, 1:1 v/v) at room temperature and a small amount of CuI was added as the catalyst. After the reaction mixture was stirred at ambient temperature overnight, it was filtered through a short pad of silica gel to remove the catalyst. The solvent was removed under reduced pressure and the crude product was separated by preparative TLC plates with hexane/CH_2Cl_2 (3:1, v/v) as eluent. The product obtained from the first-round separation was separated again with preparative TLC plates using hexane/ethyl acetate (24:1, v/v) as eluent. In this way, the title product in a pure form was obtained as viscous oil (0.122 g, 61%). IR (KBr): ν(C≡C) 2089 cm^{-1}. ^1H NMR (400 MHz, $CDCl_3$): δ = 7.56 (d, J = 7.6 Hz, 2H, Ar), 7.50 (d, J = 8.0 Hz, 2H, Ar), 7.46–7.43 (m, 4H, Ar), 7.36–7.25 (m, 8H, Ar), 6.98 (t, J = 7.6 Hz, 4H, Ar), 6.82 (t, J = 7.6 Hz, 2H, Ar), 1.90 (t, J = 8.4 Hz, 8H, C_8H_{17}), 1.83–1.76 (m, 24H, PEt_3), 1.28–0.88 (m, 76H, PEt_3 and

C_8H_{17}), 0.83 (t, J = 7.2 Hz, 12H, C_8H_{17}), 0.63 ppm (br, 8H, C_8H_{17}). ^{13}C NMR (100.3 MHz, $CDCl_3$): δ = 156.23, 150.77, 142.11, 139.11, 136.97, 131.33, 129.92, 128.56, 127.31, 126.55, 125.31, 121.27, 120.33, 119.53, 119.27, 119.21 (Ar), 114.44, 111.48, 107.30 (C≡C) 54.79 (quat. C), 40.37, 31.78, 30.10, 29.30, 29.29, 23.71, 22.58, 14.10 (C_8H_{17}), 15.05, 8.06 ppm (PEt_3). ^{31}P NMR (161.9 MHz, $CDCl_3$): δ = 10.73 ppm ($^1J_{P–Pt}$ = 2634 Hz, $PtPEt_3$). FAB-MS: *m/z* 2090 $[M]^+$. Anal. Calcd (%) for $C_{102}H_{150}HgP_4Pt_2$: C, 58.59; H, 7.23. Found: C, 58.40; H, 7.10.

[Hg-T(C_8-F)T-Pt-T(C_8-F)T-Hg]$_1$

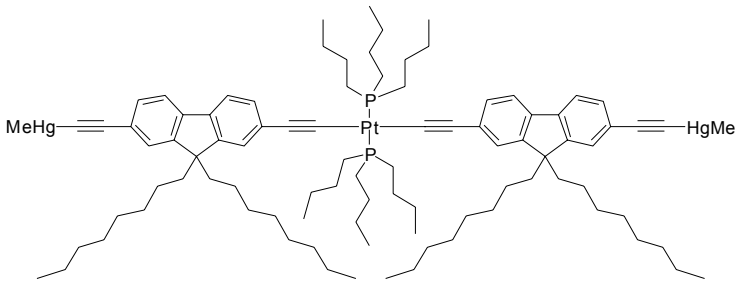

The metal precursor **[T(C_8-F)T-Pt-T(C_8-F)T]$_1$** (0.100 g, 0.068 mmol) and MeHgCl (0.043 g, 0.169 mmol) were mixed in MeOH/CH_2Cl_2 (40 mL, 1:40, v/v) to form a clear solution. Then, a basic NaOMe solution (1.0 mL, 0.2 mmol/L in MeOH) was added to the reaction mixture at room temperature. After stirring the mixture overnight at ambient temperature, it was filtered and the filtrate was allowed to evaporate slowly to form almost colorless crystals of **[Hg-T(C_8-F)T-Pt-T(C_8-F)T-Hg]$_1$** which were then collected and further recrystallized from a CH_2Cl_2/MeOH solution (0.085 g, 66%). IR (KBr): ν(C≡C) 2089 cm^{-1}. ^{1}H NMR (400 MHz, $CDCl_3$): δ = 7.53 (d, J = 7.6 Hz, 2H, Ar), 7.49 (d, J = 8.0 Hz, 2H, Ar), 7.42–7.40 (m, 4H, Ar), 7.22 (d, J = 7.6 Hz, 4H, Ar), 2.19 (m, 12H, Bu), 1.87 (m, 8H, C_8H_{17}), 1.65 (m 12H, Bu), 1.46 (m, 12H, Bu), 1.21–0.94 (m, 58H, Bu and C_8H_{17}), 0.82 (t, J = 7.2 Hz, 12H, C_8H_{17}), 0.70 (s, 6H, HgMe), 0.57 ppm

(br, 8H, C_8H_{17}). ^{13}C NMR (100.3 MHz, $CDCl_3$): δ = 150.64, 142.46, 141.44, 137.41, 131.03, 129.67, 127.99, 126.38, 125.16, 120.35, 119.44, 119.20 (Ar), 110.24, 108.77, 106.73 (C≡C) 54.77 (quat. C), 40.57, 31.78, 30.17, 29.34, 23.73, 22.57, 14.08 (C_8H_{17}), 26.37, 24.45, 23.96, 13.84 (Bu), 7.14 ppm (HgMe). ^{31}P NMR (161.9 MHz, $CDCl_3$): δ = 3.92 ppm ($^1J_{P-Pt}$ = 2350 Hz). FAB-MS: *m/z* 1904 $[M]^+$. Anal. Calcd (%) for $C_{92}H_{140}Hg_2P_2Pt$: C, 58.03; H, 7.41. Found: C, 57.88; H, 7.10.

[Au-T(C_8-F)T-Hg-T(C_8-F)T-Au]$_1$

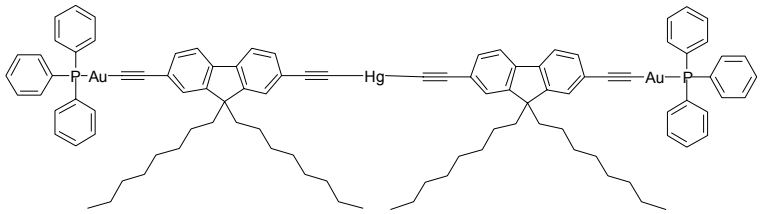

[T(C_8-F)T-Hg-T(C_8-F)T]$_1$ (0.12 g, 0.112 mmol) and $Au(PPh_3)Cl$ (0.138 g, 0.279 mmol) were combined in MeOH/CH_2Cl_2 (45 mL, 3:2 v/v) to form a clear solution. Then, basic NaOH solution (1.5 mL, 0.2 mmol/L in MeOH) was added to the reaction mixture at room temperature. After the reaction proceeded overnight at ambient temperature, the reaction mixture was concentrated. The residue was dissolved in a small amount of CH_2Cl_2 (8 mL) and poured into MeOH (50 mL). The operation was repeated three times. The pale yellow precipitate was collected by filtration and dried under vacuum (0.142 g, 64%). IR (KBr): ν(C≡C) 2140 cm^{-1}. ^1H NMR (400 MHz, $CDCl_3$): δ = 7.60–7.48 (m, 42H, Ar), 1.91 (m, 8H, C_8H_{17}), 1.23–1.01 (m, 40H, C_8H_{17}), 0.82 (t, *J* = 9.6 Hz, 12H, C_8H_{17}), 0.55 ppm (br, 8H, C_8H_{17}). ^{13}C NMR (100.3 MHz, $CDCl_3$): δ = 151.05, 150.70, 139.76, 134.23, 131.55, 131.17, 129.95, 129.40, 129.07, 127.06, 126.56, 120.82, 120.60, 119.70, 119.63, 119.29 (Ar), 107.14, 105.36, 84.77 (C≡C) 55.01 (quat. C), 40.45, 31.74, 30.16, 30.04, 29.27, 23.69, 22.56, 14.09 ppm (C_8H_{17}). ^{31}P NMR (161.9 MHz, $CDCl_3$): δ = 43.39 ppm. FAB-MS: *m/z* 1993 $[M]^+$.

Anal. Calcd (%) for $C_{102}H_{110}Au_2HgP_2$: C, 61.49; H, 5.56. Found: C, 61.21; H, 5.34.

[Au-T(C_8-F)T-Pt-T(C_8-F)T-Au]$_1$

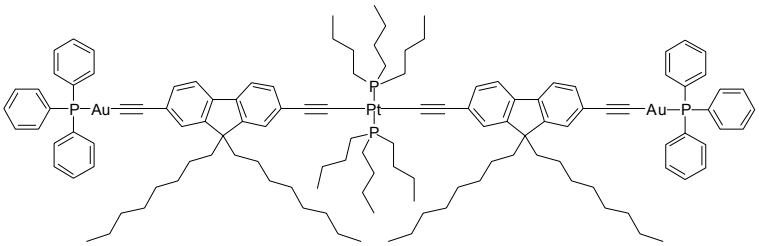

[T(C_8-F)T-Pt-T(C_8-F)T]$_1$ (0.11 g, 0.075 mmol) and Au(PPh_3)Cl (0.093 g, 0.186 mmol) were added to a mixture of MeOH/CH_2Cl_2 (45 mL, 3:2 v/v) to form a clear solution. NaOMe solution (1.1 mL, 0.2 mmol/L in MeOH) was added to the reaction mixture at room temperature. After the reaction proceeded at ambient temperature overnight, the reaction mixture was concentrated. The residue was dissolved in a small amount of CH_2Cl_2 (6 mL) and poured into MeOH (40 mL). The operation was repeated three times. The pale yellow precipitate was collected by filtration and dried under vacuum (0.12 g, 63%). IR (KBr): ν(C≡C) 2092 cm^{-1}. ^{1}H NMR (400 MHz, $CDCl_3$): δ = 7.60–7.48 (m, 38H, Ar), 7.23–7.21 (m, 4H, Ar), 2.20 (m, 12H, PBu_3), 1.90–1.86 (m, 8H, C_8H_{17}), 1.67 (br, 12H, PBu_3), 1.50–1.46 (m, 12H, PBu_3), 1.20–0.91 (m, 58H, PBu_3 and C_8H_{17}), 0.82 (m, 12H, C_8H_{17}), 0.56 ppm (br, 8H, C_8H_{17}). ^{31}P NMR (161.9 MHz, $CDCl_3$): δ = 3.85 ($^1J_{P-Pt}$ = 2356 Hz, PBu_3), 43.47 ppm (PPh_3). FAB-MS: *m/z* 2390 [M^+]. Anal. Calcd (%) for $C_{126}H_{164}Au_2P_4Pt$: C, 63.28; H, 6.91. Found: C, 63.10; H, 7.02.

***cis*-[Pt-T(C_8-F)T]$_n$**

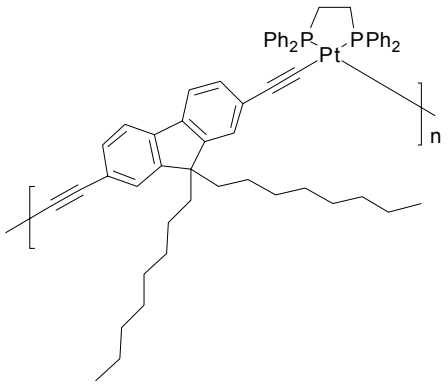

[H-T(C_8-F)T-H]$_1$ (0.055 g, 0.126 mmol) and *cis*-[$PtCl_2$(dppe)] (0.083 g, 0.126 mmol) were mixed in NEt_3/CH_2Cl_2 (40 mL, 1:10, v/v) at room temperature in the presence of a small amount of CuI (3 mg). After the reaction mixture was stirred at ambient temperature overnight, it was filtered through a short silica gel pad to remove the catalyst and the insoluble solid. The filtrate was concentrated and poured into MeOH (50 mL). The polymer powder was collected, washed with hexane and dried under vacuum (0.097 g, 75%). IR (KBr): ν = 2108 cm^{-1} (C≡C). ^{1}H NMR (400 MHz, $CDCl_3$): δ = 8.09–7.99 (br, 8H, Ar), 7.52–7.28 (br, 16H, Ar), 6.99–6.84 (m, 2H, Ar), 2.45–2.47 (d, br, 4H, $PtPCH_2CH_2PPt$), 1.80–1.75 (br, 4H, C_8H_{17}), 1.31–1.08 (m, 20H, C_8H_{17}), 0.83–0.77 (m, 6H, C_8H_{17}), 0.50 ppm (br, 4H, C_8H_{17}). ^{31}P NMR (161.9 MHz, $CDCl_3$): δ = 41.80 ppm ($^1J_{P-Pt}$ = 2282 Hz). Anal. Calcd (%) for $C_{59}H_{64}P_2Pt$: C, 68.79; H, 6.26. Found: C, 68.55; H, 6.08.

[Pd-T(C_8-F)T]$_n$

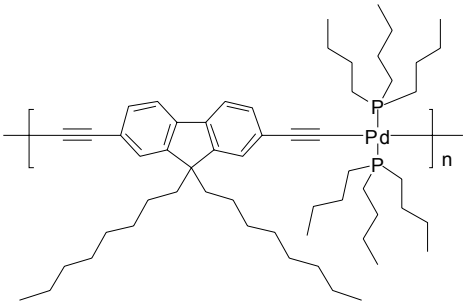

[H-T(C_8-F)T-H]$_1$ (0.080 g, 0.183 mmol) and *trans*-[$PdCl_2(PBu_3)_2$] (0.106 g, 0.183 mmol) were

added to a mixture of NEt_3/CH_2Cl_2 (50 mL, 1:1 v/v) at room temperature. A small amount of CuI was added to the reaction mixture as the catalyst for the polymerization. After the reaction mixture was stirred at ambient temperature overnight, it was filtered through a short silica gel pad. The filtrate was concentrated and poured into MeOH (50 mL). The polymer was precipitated out as a yellow-orange solid which was washed with hexane and dried under vacuum (0.11 g, 65%). IR (KBr): ν(C≡C) 2107 cm^{-1}. ^1H NMR (400 MHz, $CDCl_3$): δ = 7.50 (br, 4H, Ar), 7.25 (br, 2H, Ar), 2.12–0.60 ppm (m, 88H, PBu_3 and C_8H_{17}). ^{13}C NMR (100.3 MHz, $CDCl_3$): δ = 151.25, 141.26, 131.64, 126.91, 124.86, 119.86 (Ar), 105.89, 102.25 (C≡C) 54.90 (quat. C), 40.36, 31.74, 30.04, 29.25, 23.72, 22.56, 14.05 (C_8H_{17}), 26.63, 25.19, 24.36, 13.81 ppm (PBu_3). ^{31}P NMR (161.9 MHz, $CDCl_3$): δ = 7.48 ppm (PBu_3). Anal. Calcd (%) for $C_{57}H_{94}P_2Pd$: C, 72.24; H, 10.00. Found: C, 71.99; H, 9.88.

$[T(C_8\text{-}F)T\text{-}Pt\text{-}T(C_8\text{-}F)T]_n$

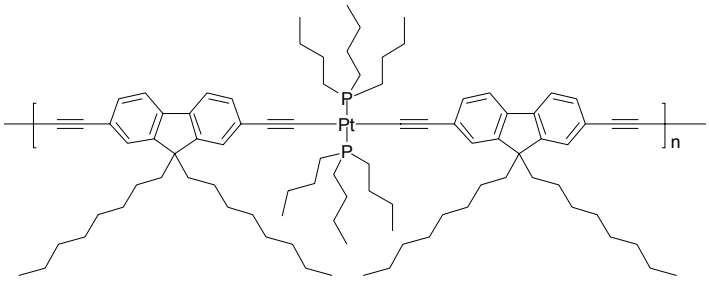

The monomer **$[T(C_8\text{-}F)T\text{-}Pt\text{-}T(C_8\text{-}F)T]_1$** (0.10 g, 0.068 mmol) was added to pyridine (8 mL) and CuCl (1.1 mg, 0.011 mmol) was added as the catalyst. The reaction mixture was stirred for 12 h at room temperature while a flow of oxygen was bubbled into it. After reaction, CH_2Cl_2 (30 mL) was added to dissolve the precipitate formed and the solution was filtered through a short silica gel pad to remove the catalyst residue. The filtrate was concentrated. The residue was dissolved in a small

amount of CH_2Cl_2 (6 mL) and poured into MeOH (50 mL). The precipitate was collected by filtration and washed with hexane. The product was obtained as a pale yellow crystalline solid. (0.095 g, 95%). IR (KBr): ν(C≡C) 2092 cm^{-1}. ^1H NMR (400 MHz, $CDCl_3$): δ = 7.59–7.42 (m, 8H, Ar), 7.26–7.25 (br, 4H, Ar), 2.20 (br, 12H, PBu_3), 1.89 (br, 8H, C_8H_{17}), 1.67 (br, 12H, PBu_3), 1.49 (m, 12H, PBu_3), 1.23–0.94 (m, 58H, C_8H_{17} and PBu_3), 0.86–0.81 (m, 12H, C_8H_{17}), 0.60 ppm (br, 8H, C_8H_{17}). ^{13}C NMR (100.3 MHz, $CDCl_3$): δ = 150.74, 142.42, 137.16, 131.21, 129.49, 128.35, 126.47, 124.97, 119.91, 119.46, 119.33, 119.15 (Ar), 110.25, 84.95, 83.28, 74.06 (C≡C) 54.83 (quat. C), 40.48, 31.78, 30.12, 29.31, 23.74, 22.59, 14.19 (C_8H_{17}), 26.37, 24.46, 23.94, 13.97 ppm (PBu_3). ^{31}P NMR (161.9 MHz, $CDCl_3$): δ = 3.96 ppm ($^1J_{P–Pt}$ = 2350 Hz). Anal. Calcd (%) for $C_{90}H_{134}P_2Pt$: C, 73.38; H, 9.17. Found: C, 73.20; H, 9.25.

[Pd-T(C_8-F)T-Pt-T(C_8-F)T]$_n$

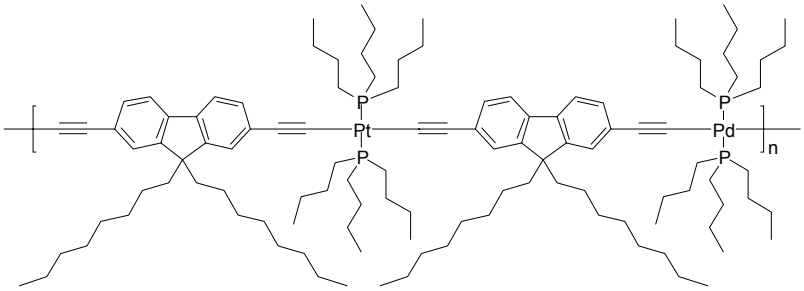

[T(C_8-F)T-Pt-T(C_8-F)T]$_1$ (0.15 g, 0.102 mmol) and *trans*-[$PdCl_2(PBu_3)_2$] (0.059 g, 0.102 mmol) were added to a mixture of NEt_3/CH_2Cl_2 (40 mL, 1:1 v/v) at room temperature. A small amount of CuI was added to the reaction mixture as the catalyst. After the reaction mixture was stirred at ambient temperature overnight, it was filtered through a short pad of silica gel and the solvent was removed in vacuo. The residue was dissolved in a small amount of CH_2Cl_2 (6 mL) and poured into MeOH (50 mL). The precipitate was collected by filtration and washed with hexane. The product

was obtained as a yellow-orange solid (0.171 g, 85%). IR (KBr): ν(C≡C) 2095 cm^{-1}. ^{1}H NMR (400 MHz, $CDCl_3$): δ = 7.49–7.45 (m, 4H, Ar), 7.25–7.22 (m, 8H, Ar), 2.22–2.07 (m, 24H, $PtPBu_3$ and $PdPBu_3$), 1.86 (br, 8H, C_8H_{17}), 1.67–1.41 (m, 48H, $PtPBu_3$ and $PdPBu_3$), 1.25–0.86 (m, 76H, C_8H_{17}, $PtPBu_3$ and $PdPBu_3$), 0.85–0.81 (m, 12H, C_8H_{17}), 0.62 ppm (br, 8H, C_8H_{17}). ^{13}C NMR (100.3 MHz, $CDCl_3$): δ = 150.29, 142.43, 138.41, 131.46, 129.51, 126.73, 125.14, 124.78, 119.68, 119.30, 118.93, 118.79, (Ar), 111.66, 110.26, 106.07, 100.50 (C≡C) 54.50 (quat. C), 40.72, 31.78, 30.26, 29.40, 23.79, 22.58, 14.58 (C_8H_{17}), 26.67, 25.20, 24.81, 13.85 ($PdPBu_3$), 26.37, 24.45, 23.95, 13.82 ppm ($PtPBu_3$). ^{31}P NMR (161.9 MHz, $CDCl_3$): δ = 3.85 ($^{1}J_{P–Pt}$ = 2362 Hz) ($PtPBu_3$), 7.42 ppm ($PdPBu_3$). Anal. Calcd (%) for $C_{114}H_{188}P_4PdPt$: C, 69.01; H, 9.55. Found: C, 68.78; H, 9.64.

[Pd-T(C_8-F)T-Hg-T(C_8-F)T]$_n$

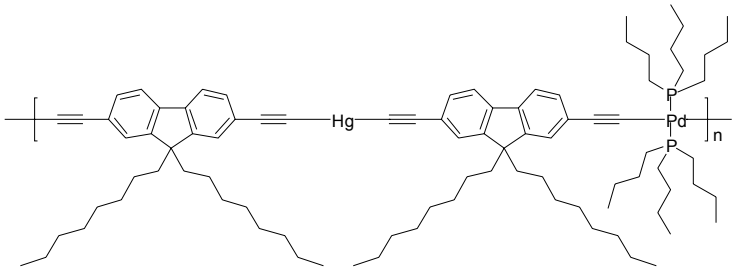

[T(C_8-F)T-Hg-T(C_8-F)T]$_1$ (0.15 g, 0.140 mmol) and *trans*-[$PdCl_2(PBu_3)_2$] (0.081 g, 0.140 mmol) were added to a mixture of NEt_3/CH_2Cl_2 (40 mL, 1:1 v/v) at room temperature. A small amount of CuI was added to the reaction mixture as the catalyst. After the reaction mixture was stirred at ambient temperature overnight, it was filtered through a short pad of silica gel to remove the catalyst. The solvent was removed under reduced pressure. The residue was dissolved in a small amount of CH_2Cl_2 (6 mL) and poured into MeOH (50 mL). The precipitate was collected by filtration and washed with hexane. The product was obtained as a yellow solid (0.175 g, 80%). IR (KBr): ν(C≡C) 2090 cm^{-1}. ^{1}H NMR (400 MHz, $CDCl_3$): δ = 7.52–7.48 (m, 8H, Ar), 7.27–7.22 (m, 4H, Ar), 2.11 (m,

12H, PBu_3), 1.96 (br, 8H, C_8H_{17}), 1.67 (br, 12H, PBu_3), 1.46 (m, 12H, PBu_3), 1.21–0.92 (m, 58H, C_8H_{17} and PBu_3), 0.84 (m, 12H, C_8H_{17}), 0.62 ppm (br, 8H, C_8H_{17}). ^{13}C NMR (100.3 MHz, $CDCl_3$): δ = 151.26, 150.80, 141.17, 131.58, 129.71, 126.92, 124.78, 120.85, 120.23, 119.70, 119.50, 118.95 (Ar), 109.40, 105.90, 95.28, 83.53 (C≡C) 55.25 (quat. C), 40.38, 31.77, 29.93, 29.29, 23.74, 22.59, 14.08 (C_8H_{17}), 26.66, 25.22, 24.38, 13.83 ppm (PBu_3). ^{31}P NMR (161.9 MHz, $CDCl_3$): δ = 7.53 ppm (PBu_3). Anal. Calcd (%) for $C_{90}H_{134}HgP_2Pd$: C, 68.20; H, 8.52. Found: C, 68.01; H, 8.33.

[Hg-T(C_8-F)T-Pt-T(C_8-F)T]$_n$

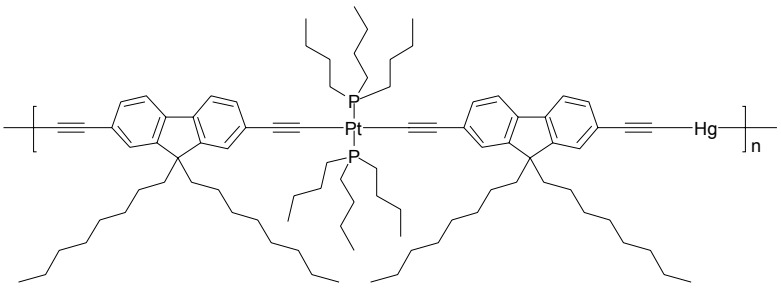

[T(C_8-F)T-Pt-T(C_8-F)T]$_1$ (0.150 g, 0.102 mmol) and $HgCl_2$ (0.028 g, 0.102 mmol) were dissolved in MeOH/CH_2Cl_2 (40 mL, 1:50 v/v) at room temperature. A basic NaOMe solution (1.2 mL, 0.2 mmol/L in MeOH) was added. After the reaction mixture was stirred at ambient temperature overnight, it was filtered through a short pad of silica gel to remove the insoluble solid. The solvent was removed under reduced pressure. The residue was dissolved in a small amount of CH_2Cl_2 (6 mL) and poured into MeOH (50 mL). The precipitate was collected by filtration and washed with hexane. The product was obtained as an off-white solid. (0.125 g, 73%). IR (KBr): ν(C≡C) 2093 cm^{-1}. ^1H NMR (400 MHz, $CDCl_3$): δ = 7.56–7.44 (m, 8H, Ar), 7.27–7.24 (m, 4H, Ar), 2.12 (br, 12H, Bu), 1.90 (br, 8H, C_8H_{17}), 1.66 (br, 12H, Bu), 1.49–1.47 (m, 12H, Bu), 1.21–0.93 (m, 58H, C_8H_{17} and Bu), 0.83 (m, 12H, C_8H_{17}), 0.60 ppm (br, 8H, C_8H_{17}). ^{31}P NMR (161.9 MHz, $CDCl_3$): δ = 3.96 ppm

($^1J_{P-Pt}$ = 2352 Hz). Anal. Calcd (%) for $C_{90}H_{134}HgP_2Pt$: C, 64.59; H, 8.07. Found: C, 64.45; H, 7.76.

[T(C_8-F)T-Hg-T(C_8-F)T]$_n$

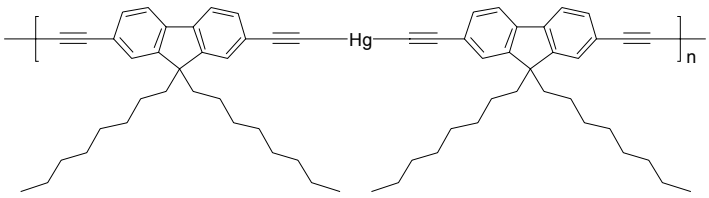

The monomer **[T(C_8-F)T-Hg-T(C_8-F)T]$_1$** (0.10 g, 0.093 mmol) was added to pyridine (8 mL) and CuCl (1.5 mg 0.015 mmol) was added as the catalyst. The reaction mixture was stirred for 12 h at ambient temperature while a flow of oxygen was bubbled through it. After the reaction, CH_2Cl_2 (30 mL) was added and the reaction mixture was filtered through a short silica gel pad to remove the catalyst residue. The filtrate was then concentrated. The residue was dissolved in a small amount of CH_2Cl_2 (6 mL) and poured into MeOH (50 mL). The precipitate was collected by filtration and washed with hexane. The product was obtained as a pale yellow solid. (0.090 g, 90%). IR (KBr): ν(C≡C) 2141 cm^{-1}. ^{1}H NMR (400 MHz, $CDCl_3$): δ = 7.66–7.63 (m, 4H, Ar), 7.51–7.48 (m, 8H, Ar), 1.91 (br, 8H, C_8H_{17}), 1.21–1.03 (m, 40H, C_8H_{17}), 0.82–0.81 (m, 12H, C_8H_{17}), 0.57 ppm (br, 8H, C_8H_{17}). ^{13}C NMR (100.3 MHz, $CDCl_3$): δ = 151.25, 151.14, 140.95, 131.51, 131.24, 126.92, 126.72, 121.00, 120.81, 120.54, 120.21, 120.06 (Ar), 106.85, 84.50, 83.09, 74.49 (C≡C) 55.22 (quat. C), 40.22, 31.76, 29.95, 29.22, 23.70, 22.58, 14.09 ppm (C_8H_{17}). Anal. Calcd (%) for $C_{66}H_{80}Hg$: C, 73.81; H, 7.51. Found: C, 73.55; H, 7.70.

X-ray Crystallographic Details. Good-quality crystals of the samples were grown at room temperature by slow evaporation of their solutions in a CH_2Cl_2/hexane mixture. Geometric and intensity data were collected at 293 K using graphite-monochromated Mo–Kα radiation (λ = 0.71073 Å) on a Bruker Axs SMART 1000 CCD diffractometer. The collected frames were processed with the software SAINT[3] and an absorption correction (SADABS)[4] was applied to the collected reflections. The structure was solved by the Direct methods (SHELXTL)[5] in conjunction with standard difference Fourier techniques and subsequently refined by full-matrix least-squares analyses on F^2. Hydrogen atoms were generated in their idealized positions and all non-hydrogen atoms were assigned with anisotropic displacement parameters.

Theoretical Computations. Density functional calculations at the B3LYP level were performed based on their experimental geometries from the X-ray data. The basis set used for C and H atoms was 6-31G while effective core potentials with a LanL2DZ basis set were employed for P, Hg, Pd and Pt atoms. Polarization functions were added for phosphorus (ζ_d(P) = 0.34).[6] All the calculations were carried out using the Gaussian 03 program.[7] Mulliken population analyses were done with MullPop.[8]

References:

[1] a) M. S. Khan, M. R. A. Al-Mandhary, M. K. Al-Suti, B. Ahrens, M. F. Mahon, L. Male, P. R. Raithby, C. E. Boothby, A. Köhler, *Dalton Trans.* **2003**, 74. b) S. Maruyama, X.-T. Tao, H. Hokari, T. Noh, Y. Zhang, T. Wada, H. Sasabe, H. Suzuki, T. Watanabe, S. Miyata, *J. Mater. Chem.* **1999**, *9*, 893.

[2] W.-Y. Wong, L. Liu, J.-X. Shi, *Angew. Chem. Int. Ed.* **2003**, *42*, 4064.

[3] SAINT+, ver. 6.02a, Bruker Analytical X-ray System, Inc., Madison, WI, **1998**.

[4] G. M. Sheldrick, SADABS, Empirical Absorption Correction Program; University of Göttingen, Germany, **1997**.

[5] G. M. Sheldrick, SHELXTL^{TM}, Reference manual, ver. 5.1, Madison, WI, **1997**.

[6] a) W. R. Wadt, P. J. Hay, *J. Chem. Phys.* **1985**, *82*, 284. b) P. J. Hay, W. R. Wadt, *J. Chem. Phys.* **1985**, *82*, 299.

[7] M. J. Frisch, G. W. Trucks, H. B. Schlegel, G. E. Scuseria, M. A. Robb, J. R. Cheeseman, J. A. Montgomery, T. Jr. Vreven, K. N. Kudin, J. C. Burant, J. M. Millam, S. S. Iyengar, J. Tomasi, V. Barone, B. Mennucci, M. Cossi, G. Scalmani, N. Rega, G. A. Petersson, H. Nakatsuji, M. Hada, M. Ehara, K. Toyota, R. Fukuda, J. Hasegawa, M. Ishida, T. Nakajima, Y. Honda, O. Kitao, H. Nakai, M. Klene, X. Li, J. E. Knox, H. P. Hratchian, J. B. Cross, C. Adamo, J. Jaramillo, R. Gomperts, R. E. Stratmann, O. Yazyev, A. J. Austin, R. Cammi, C. Pomelli, J. W. Ochterski, P. Y. Ayala, K. Morokuma, G. A. Voth, P. Salvador, J. J. Dannenberg, V. G. Zakrzewski, S. Dapprich, A. D. Daniels, M. C. Strain, O. Farkas, D. K. Malick, A. D. Rabuck, K. Raghavachari, J. B. Foresman, J. V. Ortiz, Q. Cui, A. G. Baboul, S. Clifford, J. Cioslowski, B. B. Stefanov, G. Liu, A. Liashenko, P. Piskorz, I. Komaromi, R. L. Martin, D. J. Fox, T. Keith, M. A. Al-Laham, C. Y. Peng, A. Nanayakkara, M. Challacombe, P. M. W. Gill, B. Johnson, W. Chen, M. W. Wong, C. Gonzalez, J. A. Pople, *Gaussian 03*, revision B05, Gaussian, Inc., Pittsburgh, PA, 2003.

[8] *MullPop*, a program written by Reinaldo Pis Diez at the National University of La Plata, Argentina.

Optical-Limiting Measurements. To study the optical-limiting properties, the Z-scan measurements were performed with a Q-switched Nd:YAG laser at the repetition rate of 10 Hz. The arrangement of the system is shown in Figure S1. The laser was frequency doubled with an output wavelength of 532 nm with 10 ns pulse width for Gaussian mode by a frequency double crystal (FDC). The laser beam was then split into two beams by a beam splitter (BS). One was used as the reference beam, which was received by a detector (D_1), the other was for the sample measurement and it was focused with a lens (L_1, f = 20 cm). After transmitting through the sample (S), the light beam entered another detector (D_2). The sample to be measured was moved along a rail to change the incident irradiance on it. The incident and transmitted energies were detected simultaneously by the two detectors D_1 and D_2 (LPE-1A) individually. The performance of each of our samples was measured as an 92% transmitting solution at 532 nm in CH_2Cl_2 in a 1 mm quartz cell. Experiments with CH_2Cl_2 alone afforded no detectable optical-limiting effect, indicating that the solvent contribution is negligible.

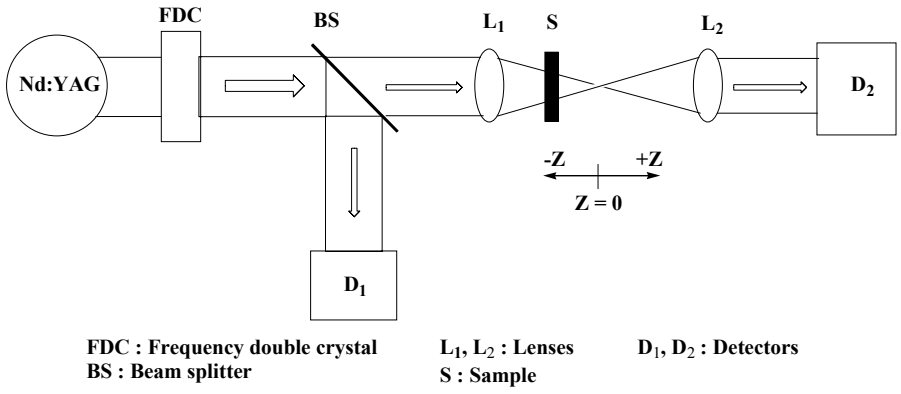

Figure S1. Experimental set-up for the measurement of optical-limiting properties.

Mathematical treatments governing the RSA process. It can be assumed that the molecular energy levels of the metallaynes could be reduced to a three-level system with no saturation, diffusion, or recombination during the pulse. Thus we neglected all excitations higher than the first singlet excitation and assumed that the intersystem crossing rate was fast (compared with the pulse duration) and that all of the initially excited charges are in the lowest triplet state. Excitation of the first triplet state then leads to excited-state absorption. The equations governing the absorption are

$$\frac{dI}{dz} = -\alpha I - \sigma_{ex} N(t) I \qquad (1)$$

$$\frac{dN}{dz} = \frac{\alpha I}{\hbar\omega} \qquad (2)$$

where I is the input laser pulse intensity, α is the linear absorption coefficient, σ_{ex} is the excited-state cross section, N is the number density of molecules in the excited state, and ω is the angular frequency of the laser. Equations (1) and (2) can be combined to get (3):

$$\frac{dI}{dz} = -\alpha I - \frac{\sigma_{ex}\alpha I}{\hbar\omega} \int_{-\infty}^{t} I(t')dt' \qquad (3)$$

Solving the equation for the fluence and integrating over the spatial extent of the laser pulse, the normalized energy transmission T for RSA can be obtained as

$$T = \ln(1 + \frac{q_0}{1+x^2}) / (\frac{q_0}{1+x^2})$$

$$q_0 = \frac{\sigma_{ex} F_0(r=0)\alpha L_{eff}}{2\hbar\omega} \qquad (4)$$

where $x = Z/Z_0$, Z is the distance of the sample from the focus, $L_{eff} = [1 - \exp(-\alpha L)]/\alpha$, and F_0 (r = 0) is the on-axis fluence at the focus.

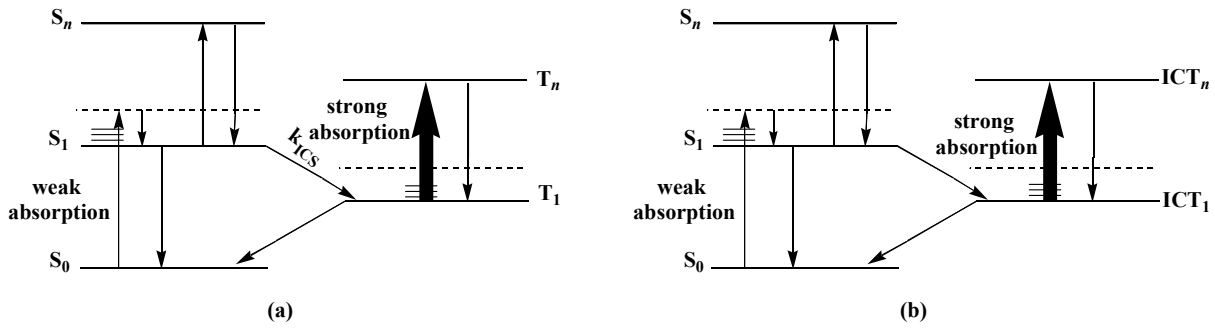

Figure S2. Energy level diagrams for the five-leveled reverse saturable absorption (RSA) optical-limiting mechanisms.

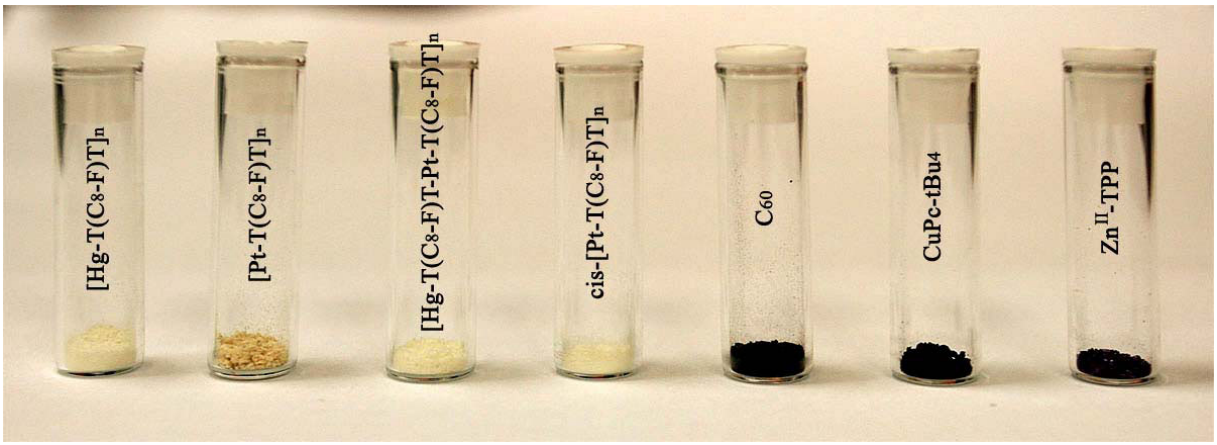

Figure S3. The sample colors of different materials in the solid state.

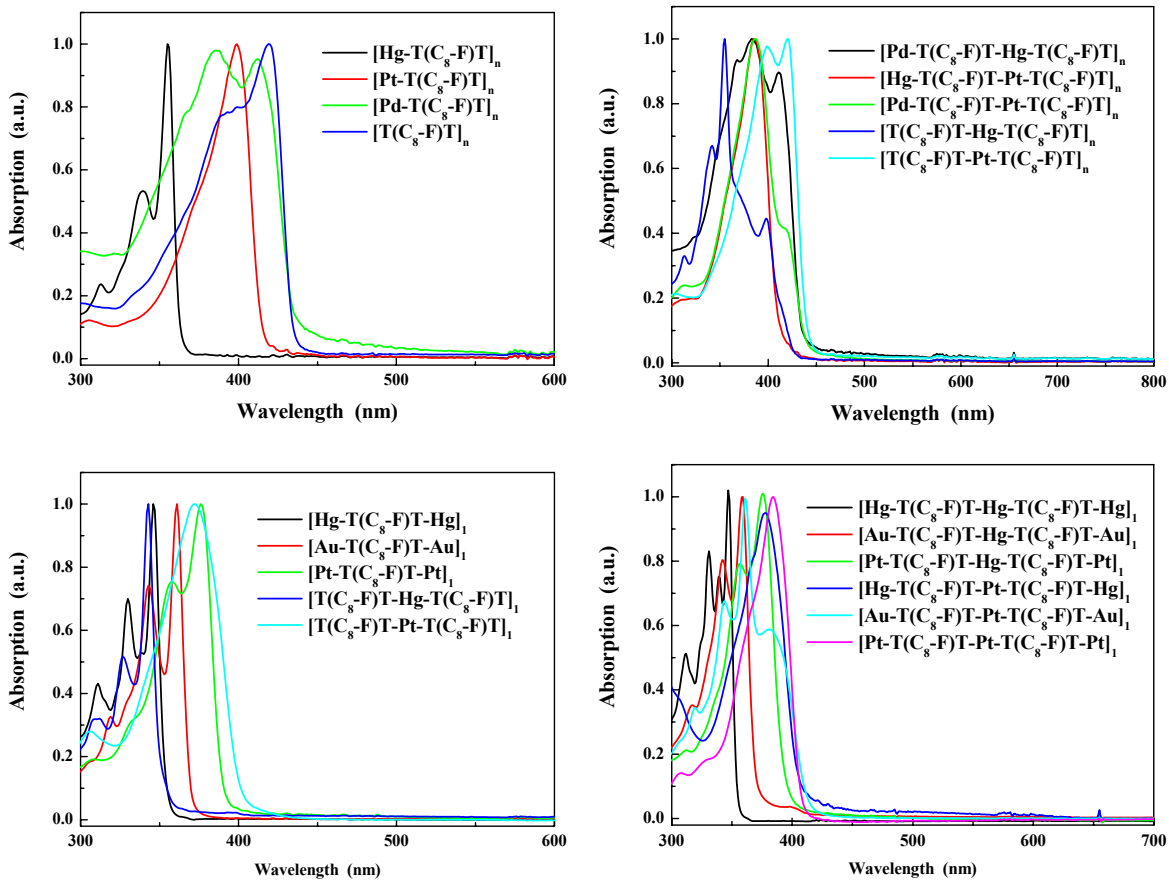

Figure S4. Linear absorption spectra of (poly)metallaynes at r.t. in CH_2Cl_2.

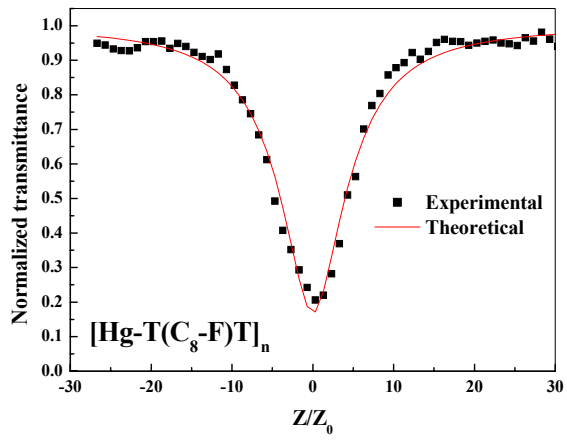
Normalized transmittance
Z/Z0
Experimental
Theoretical
[Hg-T(C8-F)T]n

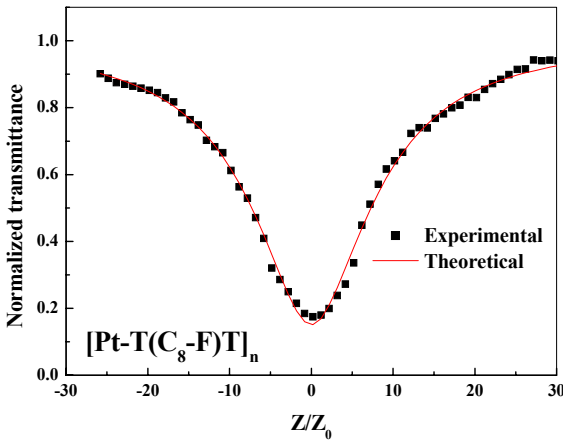
Normalized transmittance
Z/Z0
Experimental
Theoretical
[Pt-T(C8-F)T]n

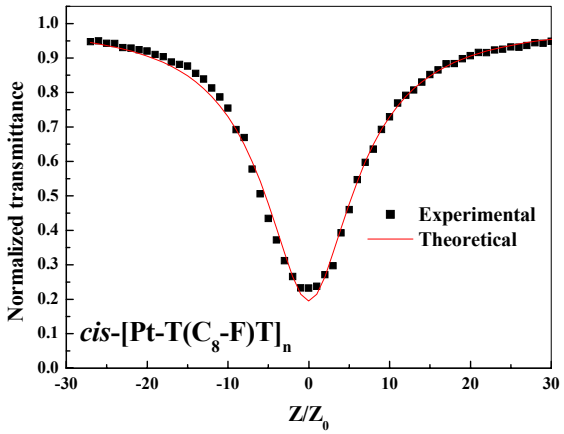
Normalized transmittance
Z/Z0
Experimental
Theoretical
cis-[Pt-T(C8-F)T]n

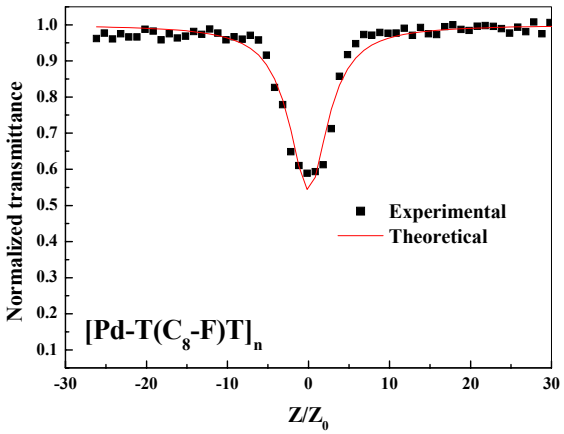
Normalized transmittance
Z/Z0
Experimental
Theoretical
[Pd-T(C8-F)T]n

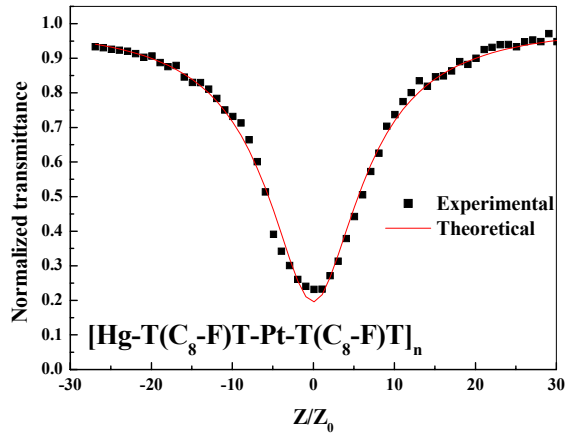
Normalized transmittance
Z/Z0
Experimental
Theoretical
[Hg-T(C8-F)T-Pt-T(C8-F)T]n

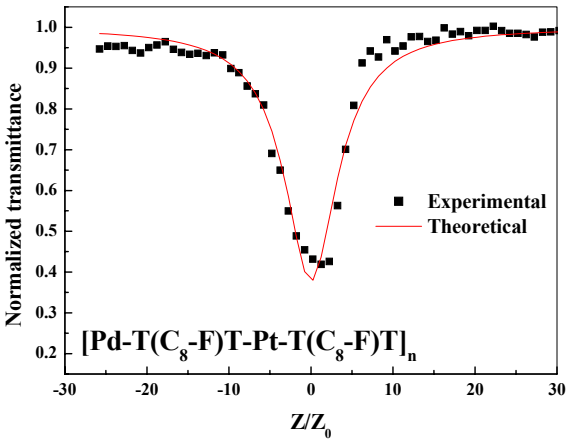
Normalized transmittance
Z/Z0
Experimental
Theoretical
[Pd-T(C8-F)T-Pt-T(C8-F)T]n

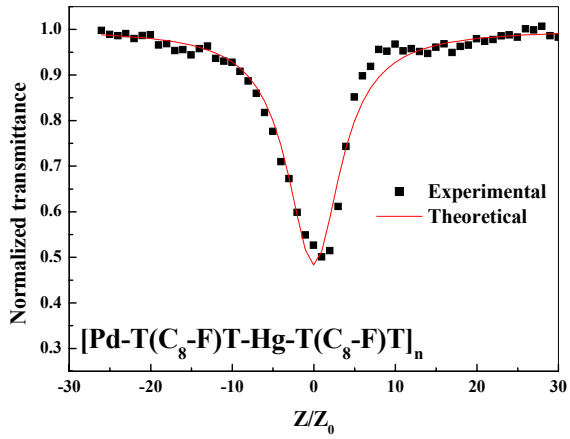
Normalized transmittance
Z/Z0
Experimental
Theoretical
[Pd-T(C8-F)T-Hg-T(C8-F)T]n

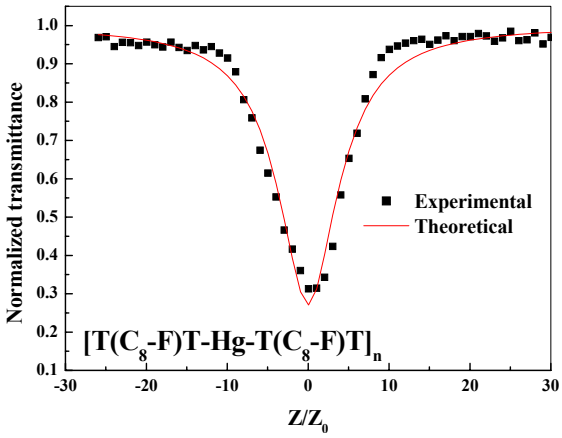
Normalized transmittance
Z/Z0
Experimental
Theoretical
[T(C8-F)T-Hg-T(C8-F)T]n

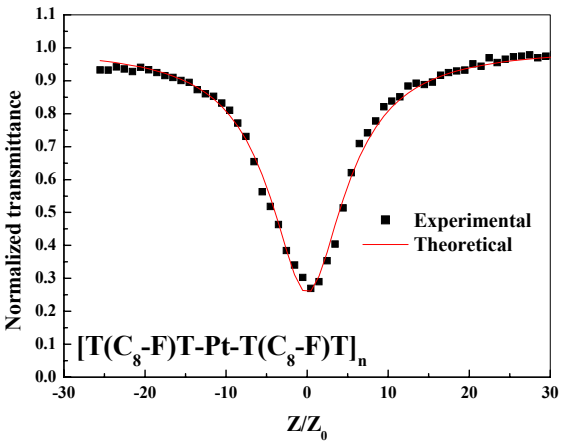
Normalized transmittance
Z/Z0
Experimental
Theoretical
[T(C8-F)T-Pt-T(C8-F)T]n

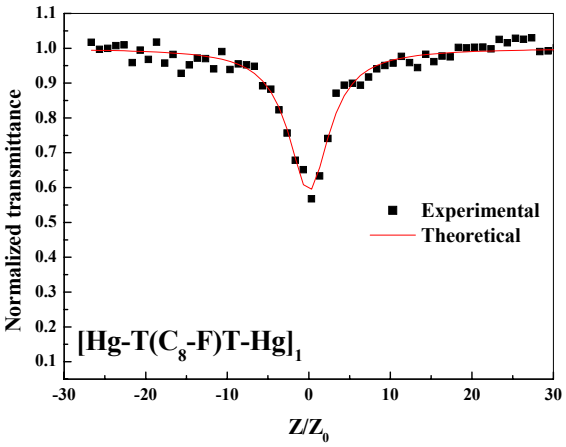
Normalized transmittance
Z/Z0
Experimental
Theoretical
[Hg-T(C8-F)T-Hg]1

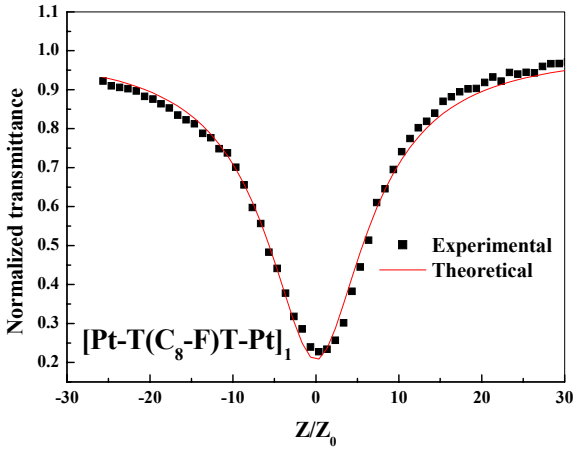
Normalized transmittance
Z/Z0
Experimental
Theoretical
[Pt-T(C8-F)T-Pt]1

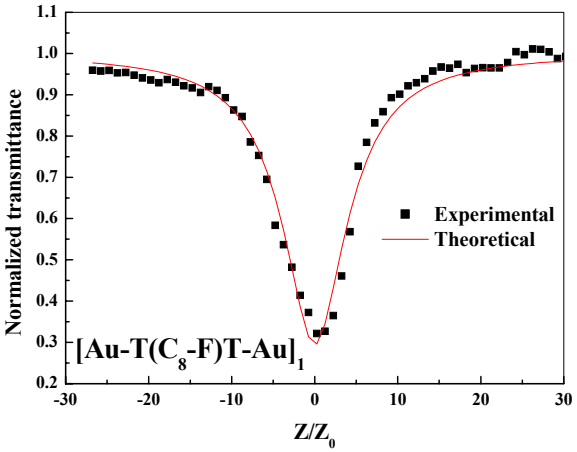
Normalized transmittance
Z/Z0
Experimental
Theoretical
[Au-T(C8-F)T-Au]1

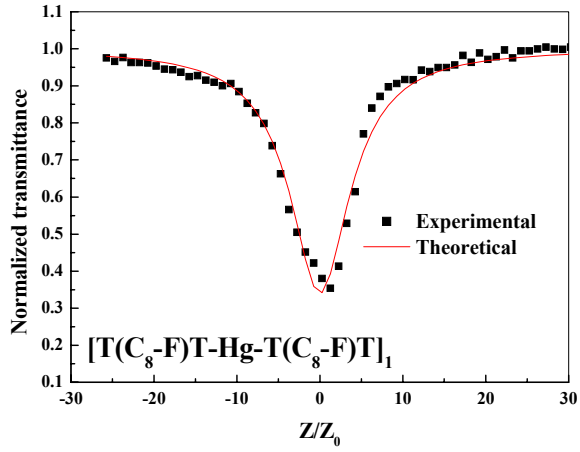
Normalized transmittance
Z/Z0
Experimental
Theoretical
[T(C8-F)T-Hg-T(C8-F)T]1

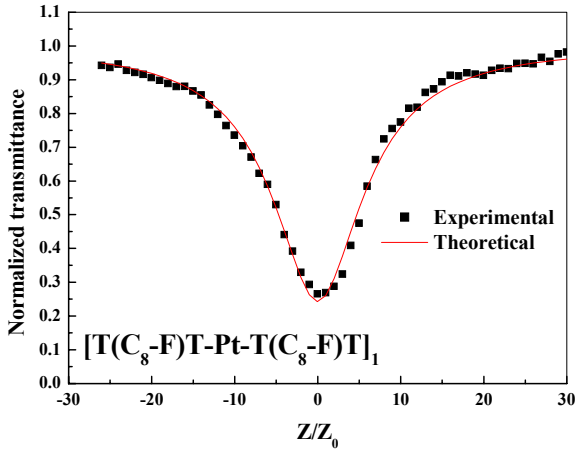
Normalized transmittance
Z/Z0
Experimental
Theoretical
[T(C8-F)T-Pt-T(C8-F)T]1

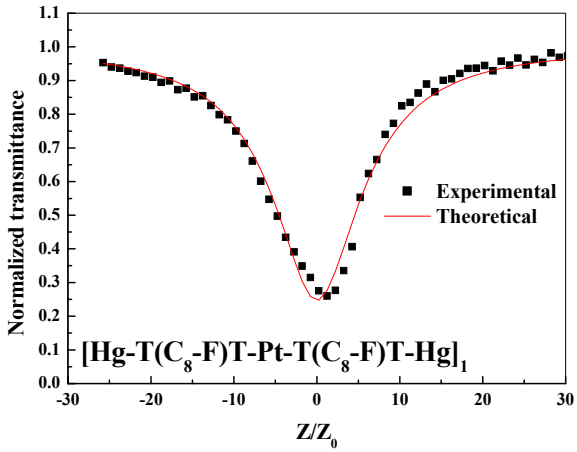
Normalized transmittance
Z/Z0
Experimental
Theoretical
[Hg-T(C8-F)T-Pt-T(C8-F)T-Hg]1

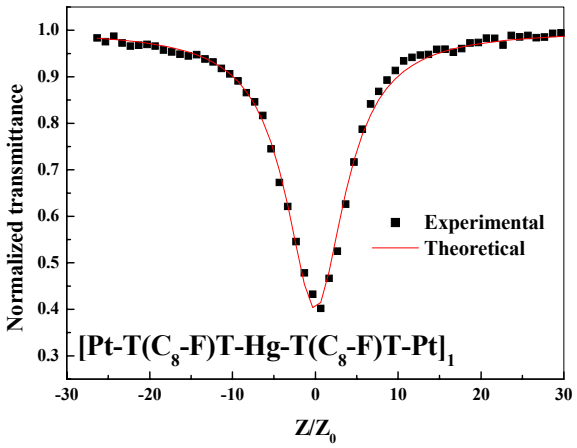
Normalized transmittance
Z/Z0
Experimental
Theoretical
[Pt-T(C8-F)T-Hg-T(C8-F)T-Pt]1

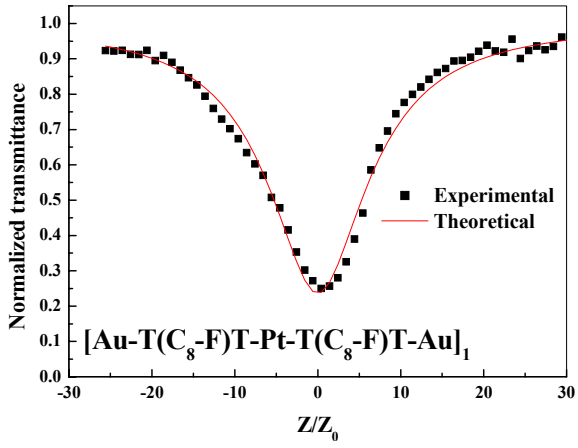
Normalized transmittance
Z/Z0
Experimental
Theoretical
[Au-T(C8-F)T-Pt-T(C8-F)T-Au]1

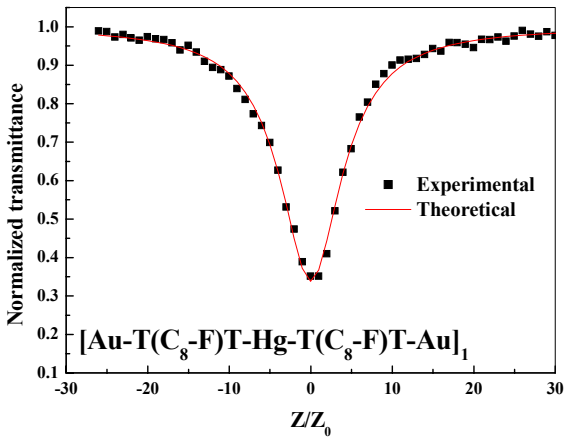
Normalized transmittance
Z/Z0
Experimental
Theoretical
[Au-T(C8-F)T-Hg-T(C8-F)T-Au]1

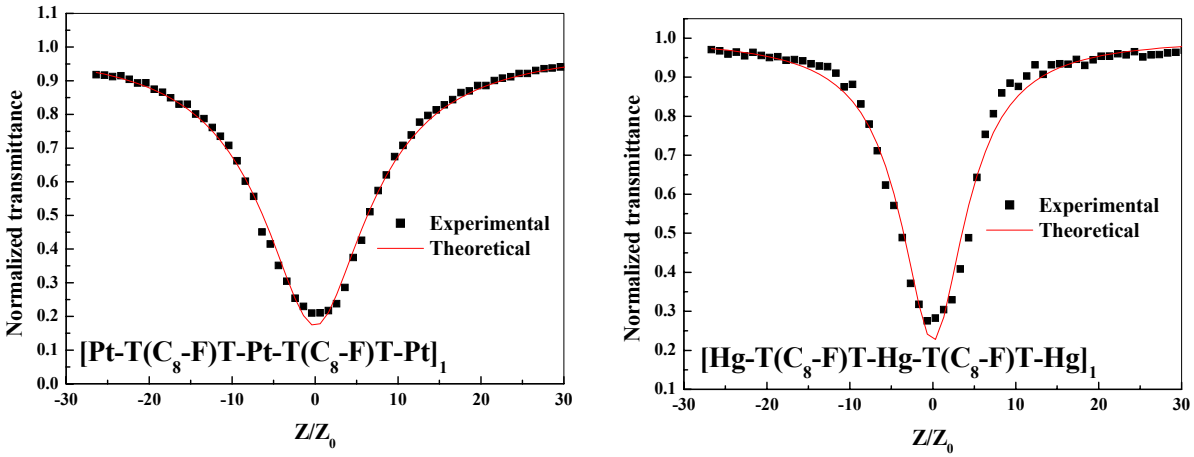

Figure S5. The Z-scan curves and their RSA numerical fits for (poly)metallaynes.

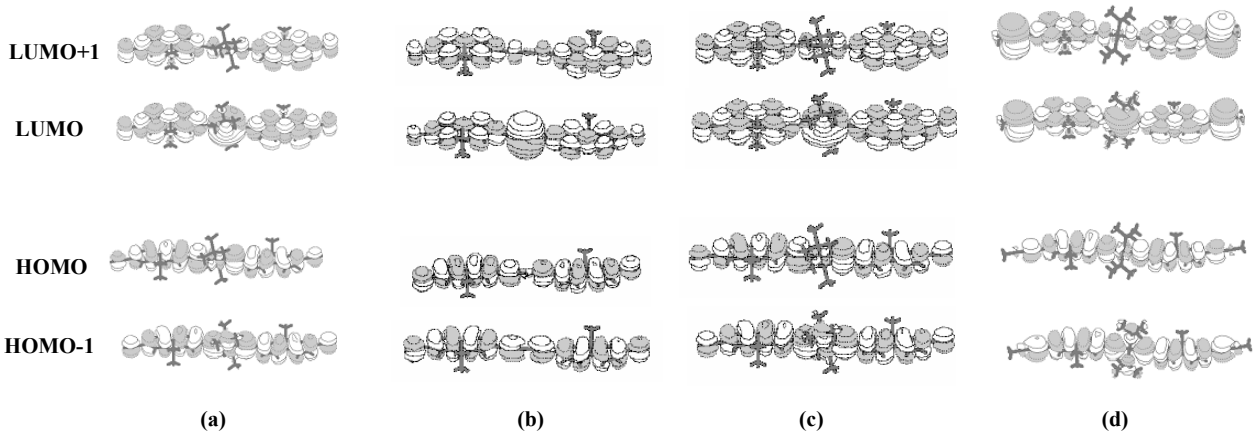

Figure S6. Spatial plots of the HOMOs and LUMOs for the model compounds of the organometallic polyynes. (a) $[T(C_8\text{-}F)T\text{-}Pt\text{-}T(C_8\text{-}F)T]_1$, (b) $[T(C_8\text{-}F)T\text{-}Hg\text{-}T(C_8\text{-}F)T]_1$, (c) $[T(C_8\text{-}F)T\text{-}Pd\text{-}T(C_8\text{-}F)T]_1$ and (d) $[Hg\text{-}T(C_8\text{-}F)T\text{-}Pt\text{-}T(C_8\text{-}F)T\text{-}Hg]_1$. For simplicity, the PBu_3 ligands were modeled by PMe_3 groups whereas the octyl chains on the fluorenyl ring were modeled by the methyl groups.

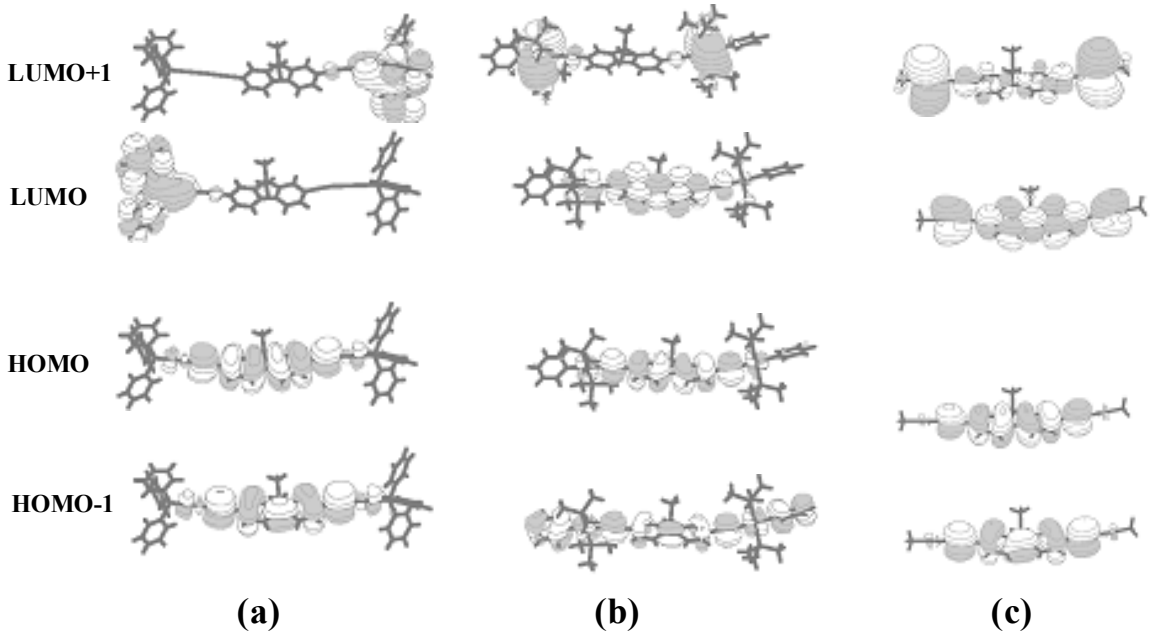

Figure S7. Spatial plots of the HOMOs and LUMOs for (a) $[Au\text{-}T(C_8\text{-}F)T\text{-}Au]_1$, (b) $[Pt\text{-}T(C_8\text{-}F)T\text{-}Pt]_1$ and (c) $[Hg\text{-}T(C_8\text{-}F)T\text{-}Hg]_1$. For simplicity, the PBu_3 ligands were modeled by PMe_3 groups whereas the alkyl chains on the fluorenyl ring were modeled by the methyl groups.

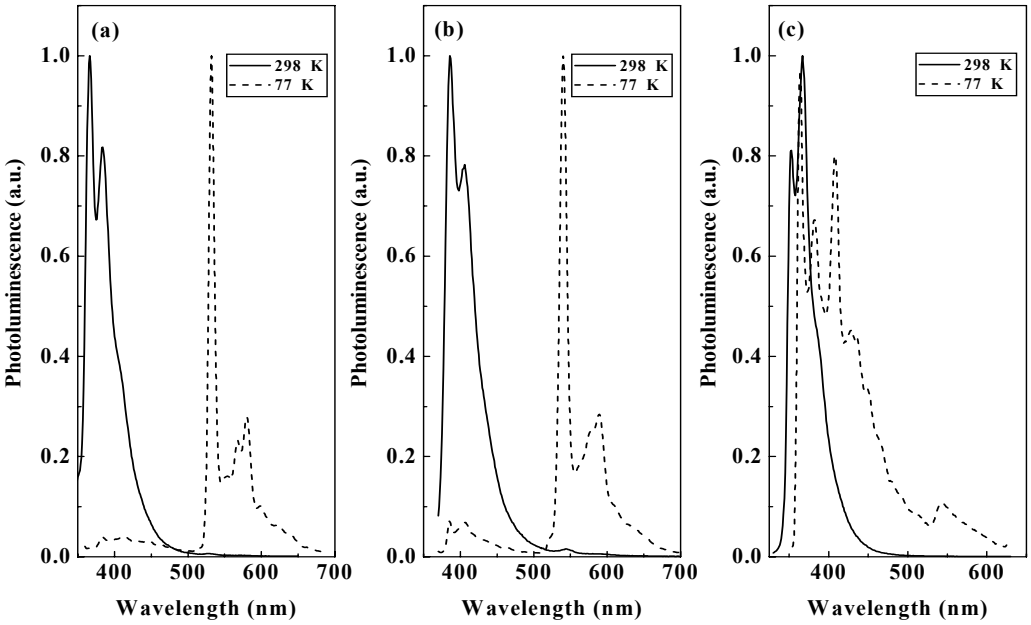

Figure S8. PL spectra at 298 K and 77 K in CH_2Cl_2 for (a) [Au-T(C_8-F)T-Au]$_1$, (b) [Pt-T(C_8-F)T-Pt]$_1$ and (c) [Hg-T(C_8-F)T-Hg]$_1$.

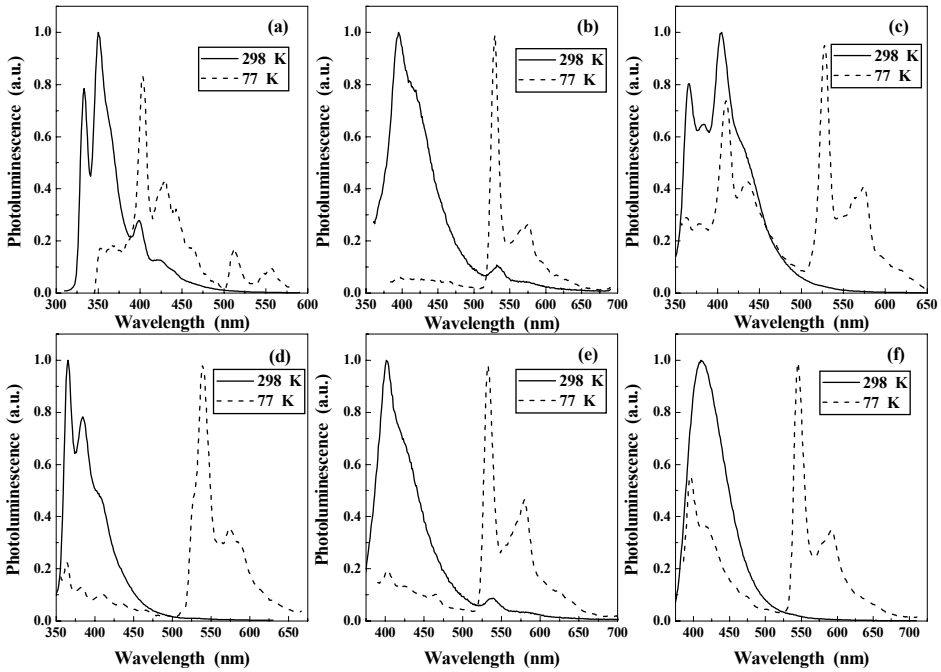

Figure S9. PL spectra at 298 K and 77 K in CH_2Cl_2 for (a) [T(C_8-F)T-Hg-T(C_8-F)T]$_1$, (b) [T(C_8-F)T-Pt-T(C_8-F)T]$_1$, (c) [Au-T(C_8-F)T-Hg-T(C_8-F)T-Au]$_1$, (d) [Au-T(C_8-F)T-Pt-T(C_8-F)T-Au]$_1$, (e) [Hg-T(C_8-F)T-Pt-T(C_8-F)T-Hg]$_1$ and (f) [Pt-T(C_8-F)T-Hg-T(C_8-F)T-Pt]$_1$.

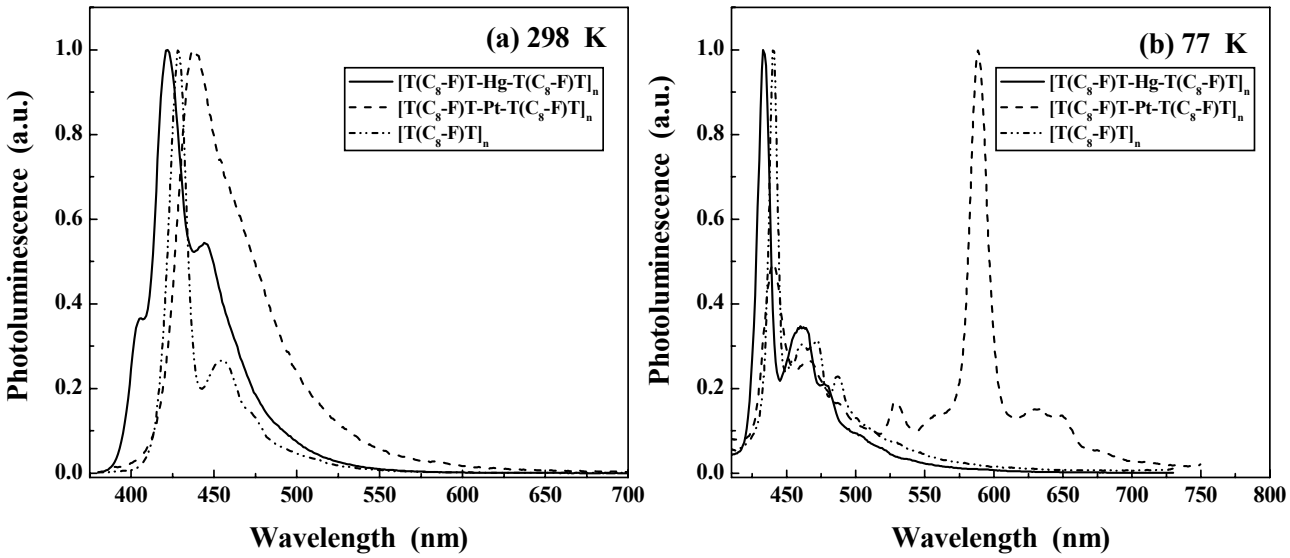

Figure S10. PL spectra for $[T(C_8\text{-}F)T\text{-}Hg\text{-}T(C_8\text{-}F)T]_n$, $[T(C_8\text{-}F)T\text{-}Pt\text{-}T(C_8\text{-}F)T]_n$ and $[T(C_8\text{-}F)T]_n$ in CH_2Cl_2 at (a) 298 K and (b) 77 K.

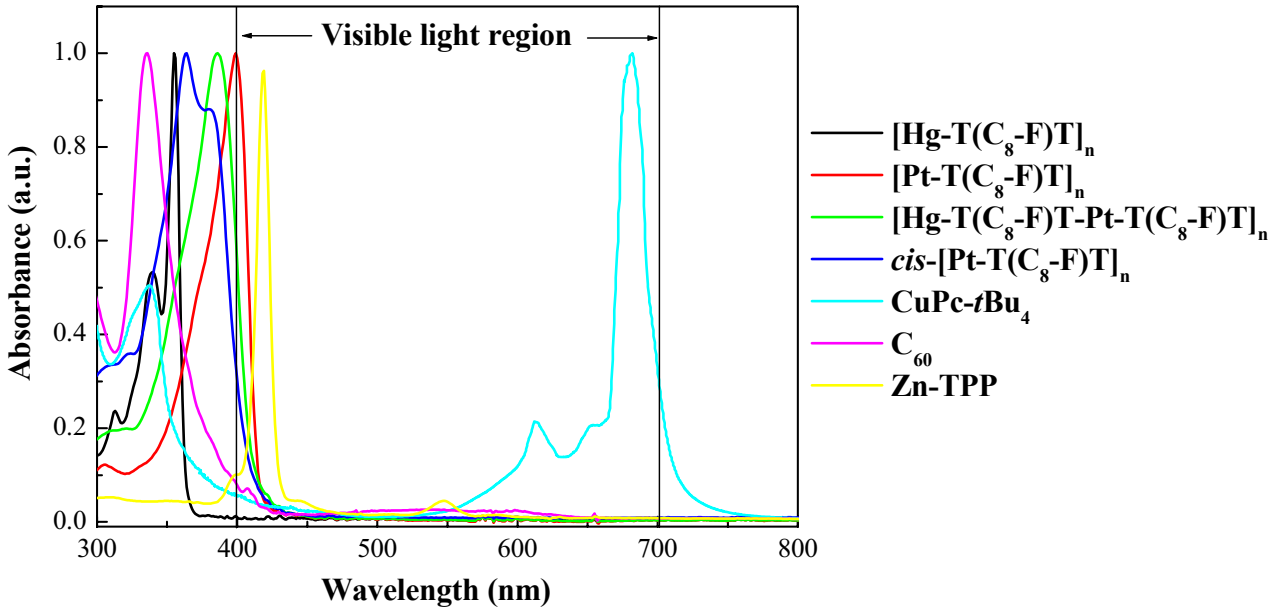

Figure S11. Comparison of the optical transparency windows of our polyplatinaynes with some state-of-the-art OPL materials.

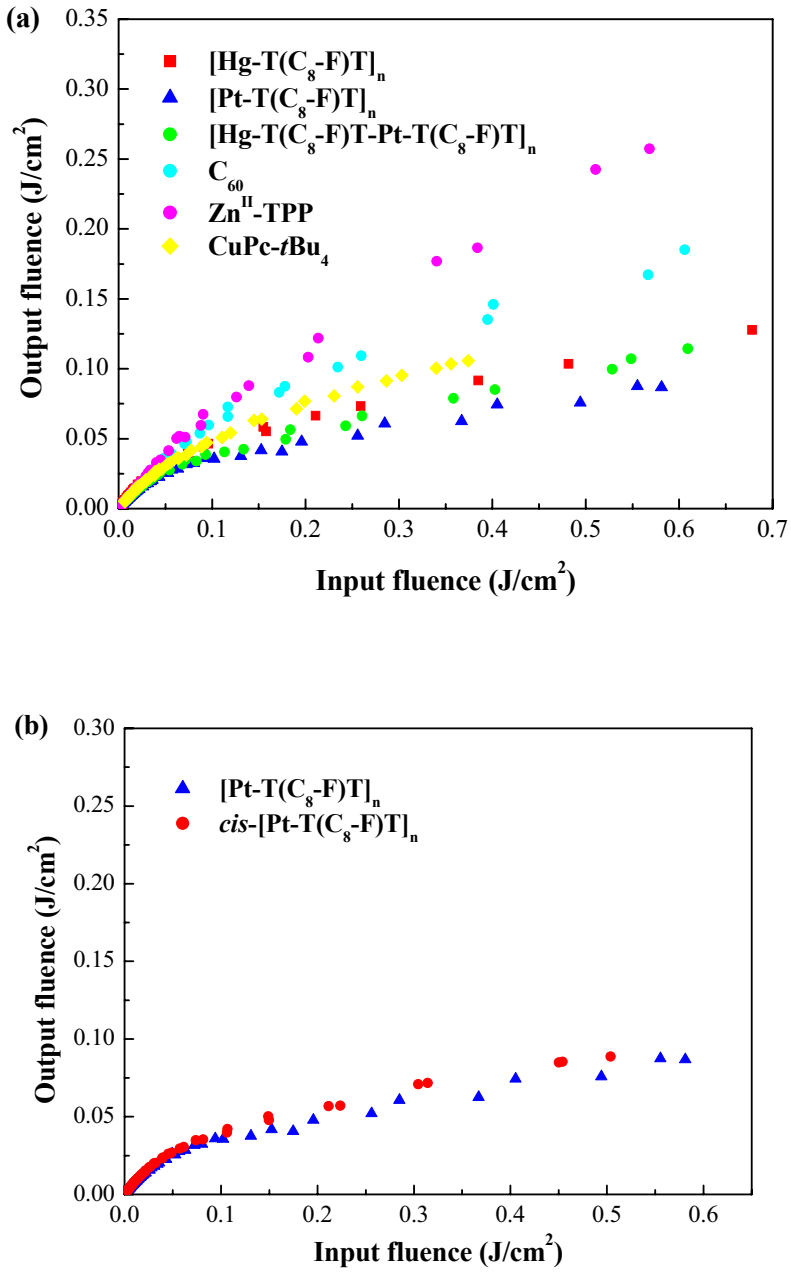

Figure S12. Comparison of the optical-limiting properties at the same linear transmittance of 92% for (a) the metallopolyynes versus state-of-the-art optical limiters and (b) **[Pt-T(C$_8$-F)T]$_n$** versus ***cis*-[Pt-T(C$_8$-F)T]$_n$**.

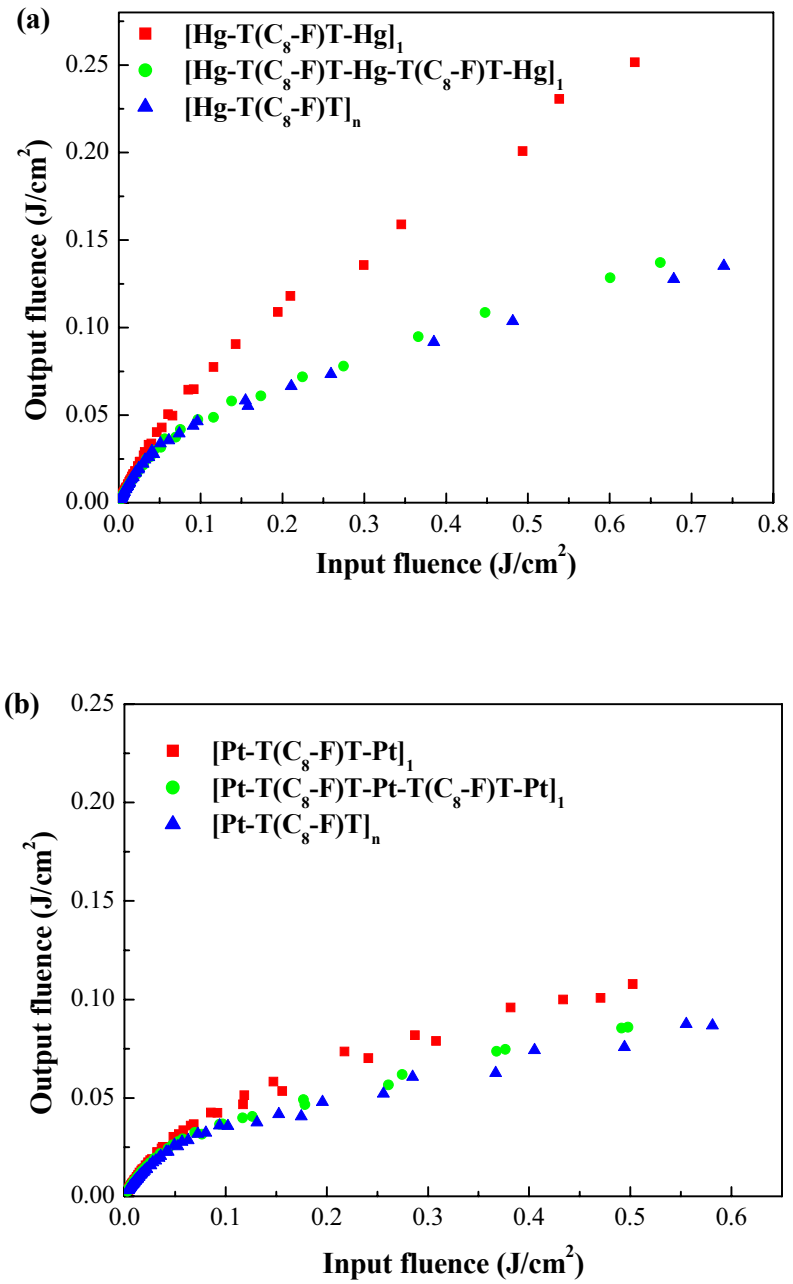

Figure S13. Comparison of the optical-limiting properties at the same linear transmittance of 92% for the (a) mercury-based alkynyl complexes and (b) platinum-based alkynyl complexes.

Table S1. Crystallographic data for selected metallayne model complexes.

	[Au-T(C_8-F)T-Au]$_1$	[Hg-T(C_8-F)T-Hg]$_1$	[T(C_8-F)-Pt-T(C_8-F)T]$_1$	[Hg-T(C_8-F)T-Pt-T(C_8-F)T-Hg]$_1$
formula	$C_{70}H_{72}Au_2Cl_2P_2$	$C_{35}H_{46}Hg_2$	$C_{90}H_{136}P_2Pt$	$C_{92}H_{140}Hg_2P_2Pt$
formula weight	1440.05	867.90	1475.02	1904.25
crystal system	triclinic	monoclinic	Monoclinic	triclinic
space group	$P\bar{1}$	Cc	$P2_1/c$	$P\bar{1}$
a (Å)	13.2656(11)	21.8830(13)	9.2061(7)	9.5394(9)
b (Å)	16.5935(14)	17.6803(13)	26.541(2)	12.9262(12)
c (Å)	16.9461(14)	9.2053(6)	17.6715(13)	20.1042(18)
α (deg)	66.7900(10)	90	90	77.171(2)
β (deg)	67.593(2)	107.840(2)	94.703(2)	78.359(2)
γ (deg)	84.370(2)	90	90	70.3490(10)
V (Å^3)	3163.5(5)	3390.3(4)	4303.3(6)	2254.4(4)
Z	2	4	2	1
D_{calcd} (g cm^{-3})	1.512	1.700	1.138	1.403
μ (mm^{-1})	4.806	9.065	1.708	5.020
F(000)	1428	1664	1568	960
θ range (deg)	1.66–25.00	1.99–28.33	1.92–25.00	1.84–25.00
reflections collected	15385	10015	21190	10824
unique reflections	10894	5992	7538	7674
R_{int}	0.0234	0.0419	0.0608	0.0369
observed reflections	8160	4357	4297	4991
no. of parameters	685	336	421	439
R1, wR2 [$I > 2.0\sigma(I)$] [a]	0.0399, 0.1023	0.0317, 0.0702	0.0497, 0.1166	0.0588, 0.1494
R1, wR2 (all data)	0.0598, 0.1137	0.0531, 0.0795	0.1059, 0.1420	0.0935, 0.1734
GoF on F^2 [b]	1.025	0.888	0.969	0.976

[a] R1 = $\Sigma\ ||F_o| - |F_c|| / \Sigma\ |F_o|$. wR2 = $\{\Sigma\ [w(F_o^2 - F_c^2)^2] / \Sigma\ [w(F_o^2)^2]\}^{1/2}$.

[b] GoF = $[(\Sigma w|F_o| - |F_c|)^2 / (N_{obs} - N_{param})]^{1/2}$.

Table S2. Selected bond lengths (Å) and angles (°) for [Au-T(C_8-F)T-Au]$_1$, [Hg-T(C_8-F)T-Hg]$_1$, [T(C_8-F)T-Pt-T(C_8-F)T]$_1$ and [Hg-T(C_8-F)T-Pt-T(C_8-F)T-Hg]$_1$.

[Au-T(C_8-F)T-Au]$_1$		[Hg-T(C_8-F)T-Hg]$_1$	
Au(1)–P(1)	2.2756(10)	Hg(1)–C(1)	2.080(11)
Au(2)–P(2)	2.2732(10)	Hg(1)–C(2)	2.045(8)
Au(1)–C(19)	1.988(4)	Hg(2)–C(18)	2.044(9)
Au(2)–C(51)	2.002(4)	Hg(2)–C(19)	2.059(9)
C(19)–C(20)	1.203(5)	C(2)–C(3)	1.186(11)
C(50)–C(51)	1.187(6)	C(17)–C(18)	1.209(13)
C(19)–Au(1)–P(1)	178.4(13)	C(1)–Hg(1)–C(2)	177.6(7)
C(51)–Au(2)–P(2)	179.66(17)	Hg(1)–C(2)–C(3)	176.8(8)
Au(1)–C(19)–C(20)	172.4(4)	C(18)–Hg(2)–C(19)	177.7(5)
Au(2)–C(51)–C(50)	176.7(5)	Hg(2)–C(18)–C(17)	176.1(12)

[T(C_8-F)T-Pt-T(C_8-F)T]$_1$		[Hg-T(C_8-F)T-Pt-T(C_8-F)T-Hg]$_1$	
Pt(1)–P(1)	2.312(2)	Pt(1)–P(1)	2.307(2)
Pt(1)–C(13)	2.012(7)	Pt(1)–C(13)	1.993(9)
C(13)–C(14)	1.199(9)	C(13)–C(14)	1.227(12)
C(44)–C(15)	1.162(11)	C(44)–C(45)	1.248(14)
		Hg(1)–C(45)	1.975(12)
		Hg(1)–C(46)	2.005(14)
C(13A)–Pt(1)–C(13)	179.996(1)	C(13)–Pt(1)–C(13A)	180.0(4)
C(13)–Pt(1)–P(1A)	92.1(2)	P(1)–Pt(1)–P(1 A)	180.0
C(13)–Pt(1)–P(1)	88.0(2)	C(13)–Pt(1)–P(1)	86.6(3)
P(1A)–Pt(1)–P(1)	179.998(1)	C(13)–Pt(1)–P(1A)	93.4(3)
		C(44)–C(45)–Hg(1)	173.0(11)
		C(45)–Hg(1)–C(46)	175.3(6)

Table S3. Structural and thermal properties of the metallopolyynes.

polymer	M_n [a]	M_w [a]	M_w/M_n	T_d (onset) (^oC) [b]	color
$[Hg\text{-}T(C_8\text{-}F)T]_n$	8880	13040	1.47	371 ± 5	white
$[Pt\text{-}T(C_8\text{-}F)T]_n$	30420	67700	2.23	368 ± 5	off-white
cis-$[Pt\text{-}T(C_8\text{-}F)T]_n$	4030	4570	1.13	406 ± 5	white
$[Pd\text{-}T(C_8\text{-}F)T]_n$	5400	7530	1.39	338 ± 5	yellow-orange
$[Hg\text{-}T(C_8\text{-}F)T\text{-}Pt\text{-}T(C_8\text{-}F)T]_n$	15700	29790	1.90	366 ± 5	off-white
$[Pd\text{-}T(C_8\text{-}F)T\text{-}Pt\text{-}T(C_8\text{-}F)T]_n$	13280	25250	1.90	368 ± 5	yellow-orange
$[Pd\text{-}T(C_8\text{-}F)T\text{-}Hg\text{-}T(C_8\text{-}F)T]_n$	4030	4520	1.12	368 ± 5	yellow
$[T(C_8\text{-}F)T\text{-}Hg\text{-}T(C_8\text{-}F)T]_n$	8030	11860	1.48	394 ± 5	off-white
$[T(C_8\text{-}F)T\text{-}Pt\text{-}T(C_8\text{-}F)T]_n$	8830	12360	1.40	406 ± 5	pale-yellow
$[T(C_8\text{-}F)T]_n$	8850	12990	1.47	408 ± 5	pale yellow

[a] Number-average (M_n) and weight-average (M_w) molecular weights were obtained by GPC against polystyrene standards. [b] By TGA under N_2 at a heating rate of 20 °C min^{-1}.

N.B. The GPC-estimated molecular weights should be cautiously viewed in light of the difficulties associated with utilizing GPC for rigid-rod polymers. GPC method does not really give absolute values of molecular weights but provides a measure of hydrodynamic volume. For rod-like polymers, appreciable differences in the hydrodynamic behavior from that of flexible polystyrene polymers would be anticipated. So, the values obtained by polystyrene calibration in GPC will likely experience a slight overestimation of the molecular weights. However, the absence of end-group NMR resonances corroborates the assertion that there is high degree of polymerization in most of these polymers.